Int J Earth Sci (Geol Rundsch) (2002) 91:799–817
DOI 10.1007/s00531-002-0260-4

ORIGINAL PAPER

André Steenken · Siegfried Siegesmund
Till Heinrichs · Bernhard Fügenschuh

Cooling and exhumation of the Rieserferner Pluton (Eastern Alps, Italy/Austria)

Received: 30 January 2001 / Accepted: 12 December 2001 / Published online: 26 March 2002

Abstract The Defereggen–Antholz–Vals (DAV) Line marks the southern border of alpine greenschist facies metamorphism within the Austroalpine basement to the south of the western Tauern window. During the Oligocene sinistral-strike slip, coeval with vertical displacement, was accompanied by the syntectonic emplacement of the Rieserferner Pluton along the north side of the fault. To the north of the DAV Line Rb/Sr as well as K/Ar-biotite cooling ages continuously increase from 16 Ma at the Rensen Pluton in the west to 30 Ma at the eastern end of the Rieserferner Pluton. Similar trends are apparent from zircon and apatite fission-track data, which increase eastward from 19 to 29 Ma, and 13 to 16 Ma, respectively. Low cooling rates allow a direct transformation into exhumation rates assuming an average geothermal gradient of 28 °C km^{-1}. The resulting exhumation rates of less than 1 mm year^{-1} do not affect the depth of isotherms in a geologically significant manner. Hence, variable cooling rates within the basement north of the DAV Line are a result of differential exhumation of individual blocks. High exhumation rates bracketed between the intrusion age of the Rieserferner Pluton at 31±3 Ma and the apatite partial annealing zone (PAZ) range between 0.4 and 0.6 mm year^{-1}, whereas final exposure takes place at reduced exhumation rates of 0.2 mm year^{-1}. East-side-down tilting of the block north of the DAV Line, as indicated by variations in exhumation rates, strongly affects the western part of the area studied between the Rensen and the Central Rieserferner Pluton whereas, further east, block rotation becomes less important. A total difference in exhumation of about 2.2 km corresponding to 5° tilting between the Western and Eastern Rieserferner, as indicated by K/Ar-biotite and zircon fission-track data, occurred before going through the PAZ for apatite fission-tracks. Furthermore, the significance of the cooling ages, especially for biotite, is tested by calculating a finite element approximation. Different numerical models indicate fast cooling of the intrusive melts prior to approaching the closure temperature of the K/Ar system in biotite.

Keywords Austroalpine basement · DAV-Line · Fission-track data · K/Ar dating · Thermal modelling

A. Steenken (✉) · S. Siegesmund · T. Heinrichs
Göttinger Zentrum für Geowissenschaften, Goldschmidstrasse 3, 37077 Göttingen, Germany
e-mail: asteenk@gwdg.de

B. Fügenschuh
Geologisch-Paläontologisches Institut, Bernoullistrasse 32, 4056 Basel, Switzerland

Introduction

Crustal scale faulting during exhumation of young orogenic belts is frequently accompanied by high angle rotations of crustal segments (Heller 1980; Rosenberg et al. 1995). Such rotations can be quantified by reconstructing the cooling history, using a number of thermo-geochronological systems with different blocking temperatures (Dodson 1973). The direct derivation of exhumation rates from the cooling history of rocks is based on a number of assumptions such as (1) the critical isotherms must have been horizontal, (2) the critical isotherms must remain at constant depth with respect to the surface and (3) the uplift rate of the rocks must be equal to the rate of erosion (Parrish 1983). Obviously, within tectonically highly active regions none of these preconditions will be fully satisfied. England and Molnar (1990) drew attention to the difference between exhumation and uplift rates. As it turns out, exhumation rates provide no information about uplift rates because the relative displacement with respect to the geoid is unknown. However, careful evaluation of cooling ages should enable us to constrain at least relative amounts of differential vertical displacement.

This study is focused on the narrow crustal segment of the Austroalpine basement between the western Tauern Window and the Southern Alps, comprising two crustal scale transpressive strike slip faults active during Alpine times: the Kalkstein–Vallarga (KV) Line (Sassi et

al. 1974; Borsi et al 1978; Guhl and Troll 1987) and the Defereggen–Antholz–Vals (DAV) Line (Borsi et al. 1973, 1978; Kleinschrodt 1978; Schulz 1989). Furthermore, the block to the north of the DAV Line includes the syntectonically emplaced Rieserferner Pluton (Mager 1985; Steenken et al. 2000). Our interest in testing and refining the published model of rotation of the crustal block north of the DAV Line (Borsi et al. 1978) involves the question whether both the fabrics and the outcrop pattern of the Rieserferner Pluton are in their primary orientation. This is particularly so because the shape of the pluton bears a certain similarity to the Bergell Pluton where a large amount of tilting has been demonstrated (Rosenberg et al. 1995).

Adding to the existing data base of K/Ar- and Rb/Sr-mica cooling ages (Borsi et al. 1973, 1978; Stöckhert 1984; Hammerschmidt 1981; Prochaska 1981) seven new K/Ar-biotite and ten new K/Ar-muscovite ages were determined in order to reconstruct differential vertical displacement before and during the intrusion of the Rieserferner Pluton. Furthermore, 24 new apatite and 12 new zircon fission-track ages, in combination with previously released fission-track data (Grundmann and Morteani 1985; Coyle 1994; Fügenschuh 1995; Stöckhert et al. 1999; Angelmaier et al. 2000), yield information on the post-intrusive exhumation history of the considered segment of the Austroalpine basement.

Beyond the above mentioned difficulties in the interpretation of cooling ages in terms of exhumation rates, K/Ar-biotite cooling ages have to be carefully evaluated whether they record true exhumation, passing the 300 °C isotherm, or reflect cooling after the emplacement of the hot magmas of the Rieserferner Pluton (Hammerschmidt 1981; Prochaska 1981). Recently published numerical models of the thermal evolution in contact metamorphic envelopes around large intrusive bodies (Bonneville and Capolsini 1999; Kosakowski et al. 1999; Siegesmund et al. 2001; Westphal et al. 2002) show excellent agreement with P–T conditions obtained from field studies. Although magmatic intrusions in fault zones are a widespread phenomenon, the complex interaction of different physical and chemical mechanisms coupled with the cooling of plutons is still poorly understood. Consequently, the correctness of the thermal model depends on the quality, amount and density of available field data. In the Rieserferner area, with its 3-D outcrop pattern, detailed studies on the contact metamorphic evolution are available (Prochaska 1981; Mager 1985; Cesare 1992, 1994, 1999), which have explored the heating of the country rock by intrusion of the hot magmas of the Rieserferner Pluton.

Geological setting

The Austroalpine basement between the western Tauern Window and the Periadriatic Line (PL) is divided into three crustal segments separated by two major Alpine crustal scale shear zones (Fig. 1). In the north, the Defereggen–Antholz–Vals (DAV)Line separates two crustal blocks with a different cooling history. Alpine metamorphism and structural reworking of Variscan basement rocks within the northern block (Stöckhert 1984; Schulz 1997; Schönhofer 1999) leading to Oligoc-

Fig. 1 Tectonic overview of the Periadriatic Line and related Alpine faults (*insert*) with (detailed) focus on the Austroalpine basement SW of the Tauern Window. Note the opposing strike slip regimes along the Puster Valley Line and the Defereggen–Antholz–Vals (*DAV*)-Line and Kalkstein–Vallarga (*KV*)-Line. The Oligocene Rieserferner Pluton exhibits a close relationship with the DAV Line bordering the pluton partly in the south

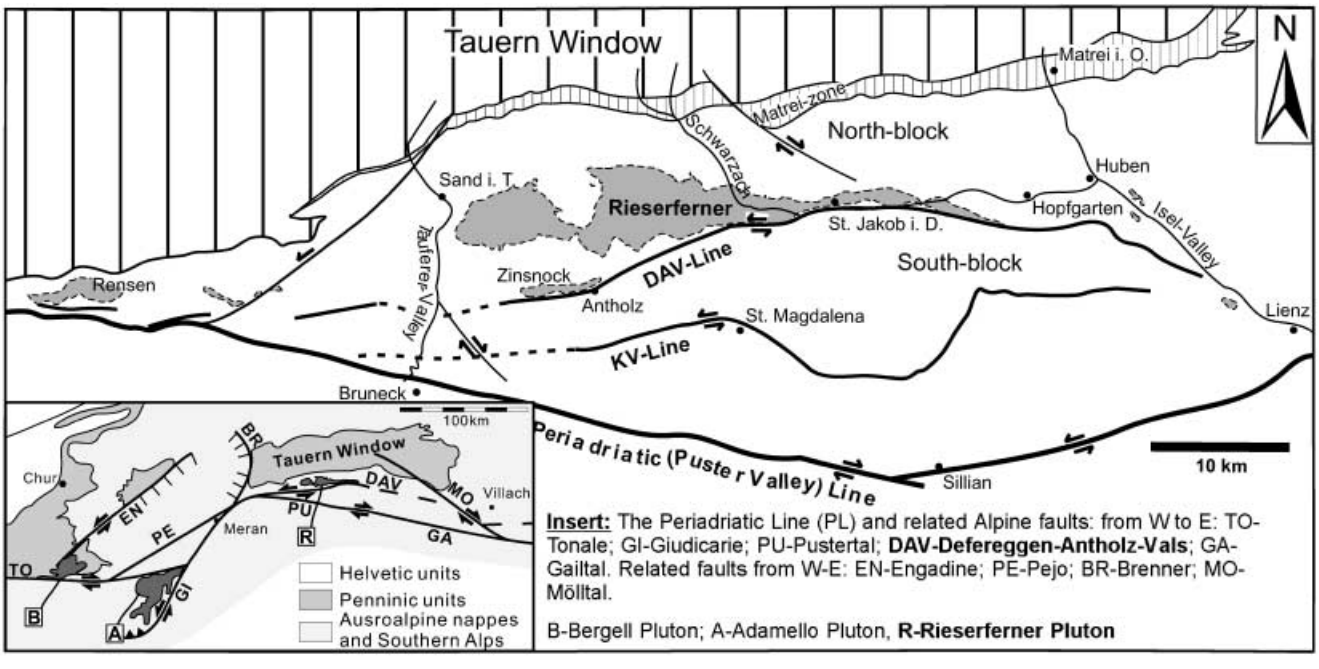

ene Rb/Sr and K/Ar-biotite cooling ages (Borsi et al. 1973, 1978; Hammerschmidt 1981) are juxtaposed against the Variscan metamorphic basement of the southern block that records a weak Alpine brittle deformation only (Schulz 1994, 1997). Furthermore, this southern block is affected by late Alpine brittle deformation along the Kalkstein–Vallarga (KV) Line (Borsi et al. 1973; Sassi et al. 1974). The continuation of both lines to the west in the Brenner Area and east across the Isel Valley is still under discussion (Hoke 1990; Stöckli 1995; Schulz 1997). A conspicuous feature of the DAV Line is the close occurrence of numerous tonalitic to granodioritic intrusions like the Rensen Pluton (31.1–31.7 Ma, Barth et al. 1989), Altenberg Pluton (Bellieni et al. 1984), Zinsnock Pluton (Mager 1985) and the sizeably E–W elongated Rieserferner Pluton (31±3 Ma, Müller et al. 2000 – recalculated after Borsi et al. 1979), which invade the Austroalpine basement to the north of the fault line.

In contrast to the dextral character of the PL, a sinistral strike-slip regime is reported for the DAV Line (Kleinschrodt 1978; Fig. 1). The integration in a regional context and the timing of movements are still controversial. Evidence for an Oligocene displacement along the DAV Line is provided by the syntectonic emplacement of the Rieserferner Pluton as indicated by the sheared contact metamorphic andalusite and textured growth of fibrolite within the mylonitic fault rocks, whereas the marginal areas of pluton, as well as the granitoid injections within the mylonitic country rock, suffer a high amount of solid-state deformation (Becke 1892; Prochaska 1981; Mager 1985; Zarske 1985; Schulz 1989, 1994; Most 1997; Mann and Scheuvens 1998; Steenken et al. 2000).

K/Ar-biotite ages in the block north of the DAV Line prove a vertical displacement across the DAV Line at around 30 Ma (Borsi et al. 1973, 1978). Additionally, Stöckhert (1984) found evidence on the base of K/Ar-muscovite ages that the DAV Line was active during the Cretaceous also. The stop of vertical offset across the DAV Line is constraint by continuous N–S increasing apatite fission-track ages (Grundmann and Morteani 1985; Coyle 1994), attesting the common pass through the apatite partial annealing zone (PAZ) of the whole basement before 22 Ma.

The problem arises from the opposing strike-slip movements along the DAV Line and the PL forming at a very acute angle during Oligocene times (Schmid et al. 1989). A possible explanation is offered by the lateral escape model of Kazmer and Kovacs (1985), which was also forwarded by Ratschbacher et al. (1991). Recently, Mancktelow et al. (2001) has drawn attention to the timing of changes in the displacement. On the basis of Rb/Sr microchrons (Müller et al. 2000) and observation of some dextral shear indications within the deformed adjacent intrusives they infer a dramatic change from transpressive sinistral to a transpressive dextral strike-slip close to 30 Ma. Consequently, sinistral strike-slip should have ceased before the beginning of dextral strike-slip along the PL. Because the timing of quartz fabric formation is hard to constrain, sinistral displacement indicated by the majority of these fabrics could easily be accommodated at an earlier stage of deformation. A late Cretaceous east–west extension has been demonstrated, for instance in the Austroalpine Ötztal–Stubai basement (Fügenschuh et al. 2000). These extensional faults are frequently accompanied by sinistral strike-slip faults that are probably related to the westward displacement of the Austroalpine nape pile (Froitzheim et al. 1997). By analogy, the Tertiary persistence of sinistral strike-slip along the DAV Line could possibly be linked with the exhumation of the Tauern gneisses during the Oligocene (Zimmermann et al. 1994).

Methods

In order to reconstruct the thermal history of a crustal section on the base of thermochronometric data closure temperatures (T_C) of the applied dating methods have to be well constrained. In the field of Rb/Sr and K/Ar mica dating the values of Purdy and Jäger (1976) are largely accepted. They suggest a T_C of 500±50 °C for the Rb/Sr-system of white-micas, while the K/Ar-system closes at 350±50 °C. In the case of biotite identical T_C at 300±50 °C for both systems are supposed.

In fission-track dating, the blocking temperature concept of Dodson (1973) is expanded and replaced by the 'partial annealing zone (PAZ)' (Wagner 1972). Particularly for apatite, track-lengths measured on confined horizontal tracks (Gleadow et al. 1986) provide further information to constrain different geological scenarios. The upper and lower temperature limits for the PAZ of apatite fission-tracks are 120 and 60 °C, respectively (e.g. Green et al. 1989).

The understanding of fission-track annealing in zircon is, up to now, still a matter of detailed research (see for example: Rahn et al. 2002a, 2002b). A large number of different estimates on the range of the PAZ exist in the literature (for a recent review see Stöckhert et al. 1999). A good compromise, also in the understanding of previously published zircon fission-track data, is the range of 240±60 °C proposed by Yamada et al. (1995).

Data acquisition

Supplementing the extensive database published during the last three decades, new K/Ar ages of white-mica and biotite, as well as zircon and apatite fission-track ages, were acquired in order to constrain the proposed model of Borsi et al. (1978) concerning the variable exhumation of the Austroalpine basement to the south of the western Tauern Window. Sample sites and distribution of the compiled thermochronometric data are presented in Figs. 2, 3, 4, 5 and 6. Tables 1 and 2 give an overview of the new results. The analytical techniques employed are briefly outlined in the appendix.

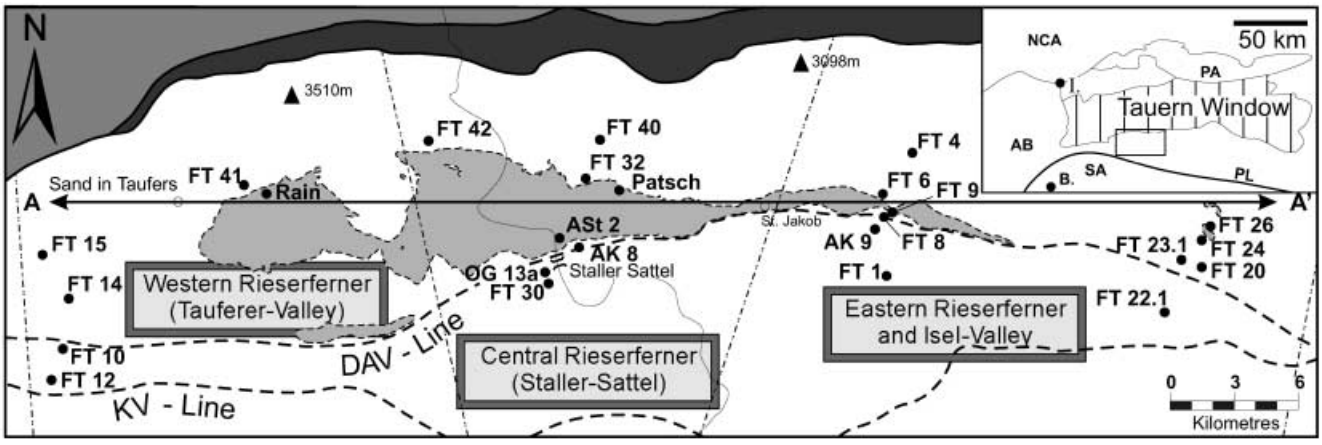

Fig. 2 Presentation of localities and designation of the collected sample material within in the Austroalpine basement SW of the Tauern Window. Also indicated is the E–W profile (*A*–*A´*) in the north of the DAV Line (cf. Fig. 8) and the selected areas for data compilation in Fig. 7

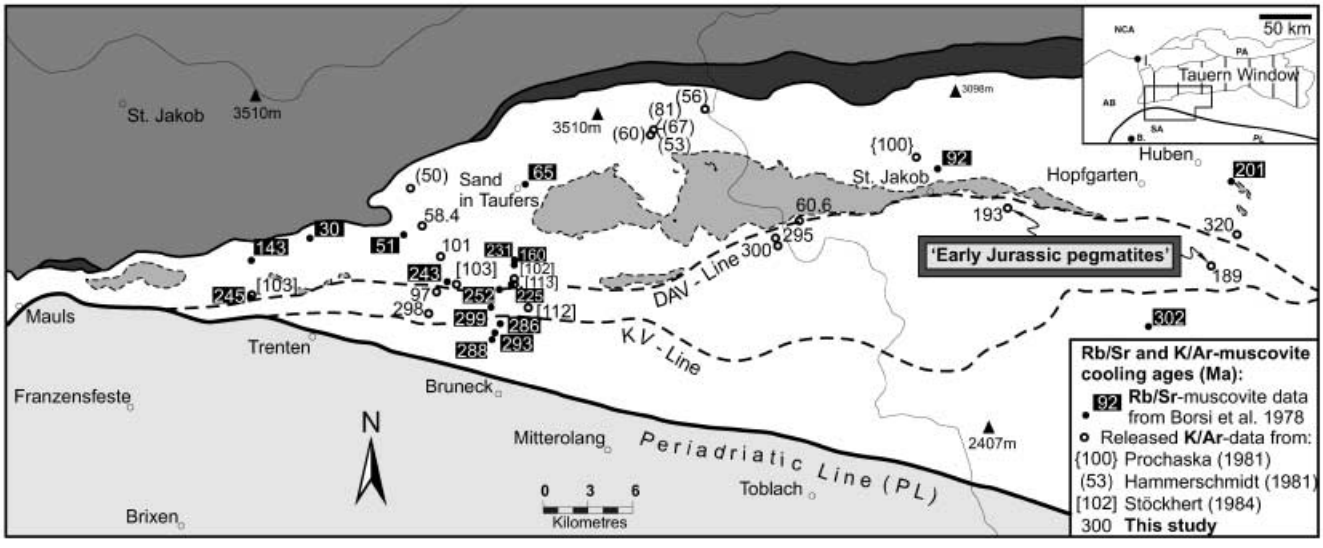

Fig. 3 Compilation of previously published Rb/Sr-muscovite ages by Borsi et al. (1979) and K/Ar-muscovite ages from earlier investigations (see *insert*), and new data. Indicated are the two analysed pegmatitic rocks from the basement in the south of the DAV Line yielding an Early Jurassic age. At least for the western pegmatite K/Ar-biotite ages in the surrounding basement rocks reflect cooling at about 280 Ma (cf. Fig. 4). Note that closure temperatures of the two data sets differ by about 150 °C between 500±50 and 350±50 °C, respectively (Purdy and Jäger 1976)

New K/Ar mica and fission-track results

The significance of Rb/Sr- and K/Ar-muscovite cooling ages

The starting point for the cooling path of the Austroalpine basement south of the western Tauern Window is established by Rb/Sr-muscovite cooling ages (Borsi et al. 1973, 1978; Hammerschmidt 1981; Prochaska 1981). The wide scatter of the data is prohibitive for a detailed interpretation. Published ages south of the DAV Line fit a narrow range between 286 and 302 Ma whereas, north of the DAV Line, the variability is much higher (Fig. 3). Cooling ages between 230–250 Ma next to the DAV Line in the west between the Rensen and Rieserferner Pluton are strongly younging towards the Tauern Window, where an age of 30 Ma is detected. Prochaska (1981) found K/Ar-muscovite cooling ages between 29.5 and 31.7 Ma in the immediate contact of the Rieserferner Pluton, which are certainly related to contact metamorphic heating during the intrusion (see below).

New K/Ar white-mica ages are mainly restricted to the block south of the DAV Line. Only along the westernmost sample traverse white-mica cooling ages are presented on both sides of the fault. Sample FT 14 from the southern part of the block north of the DAV Line yielded an age of 101±2 Ma, confirming the previously published data by Stöckhert (1984). This age is interpreted to reflect cooling after Cretaceous metamorphism (Stöckhert 1984). Further to the north, strongly decreasing K/Ar white-mica cooling ages overlap within error limits with Rb/Sr white-mica ages, suggesting rapid

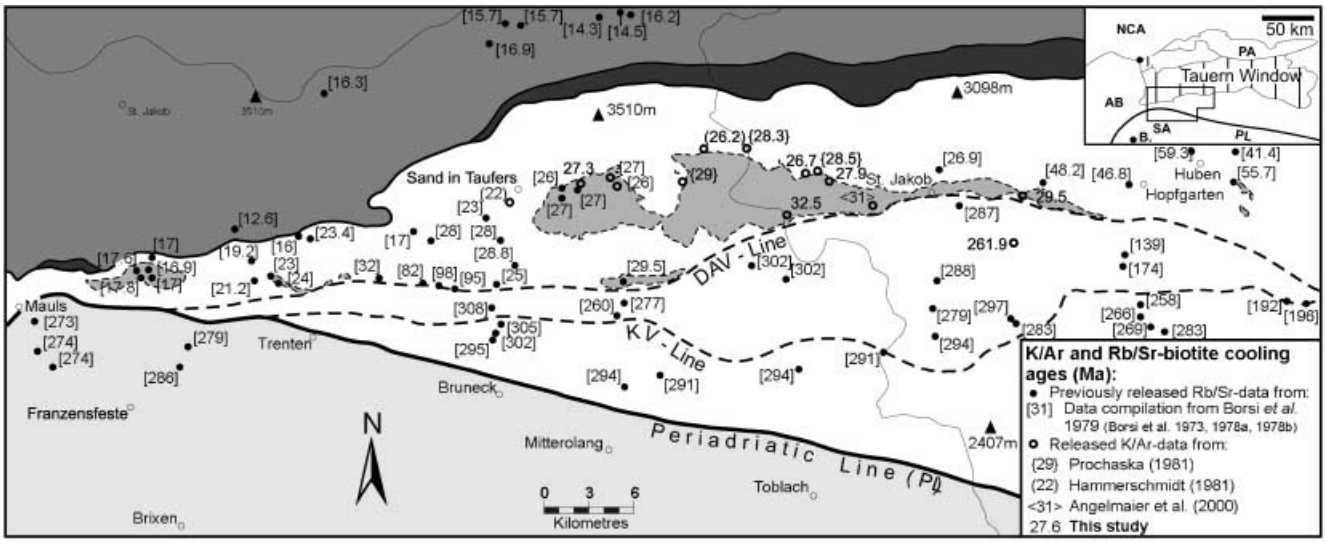

Fig. 4 Compilation of K/Ar- and Rb/Sr-biotite cooling ages from earlier investigations (see *insert*) and the new K/Ar-biotite ages

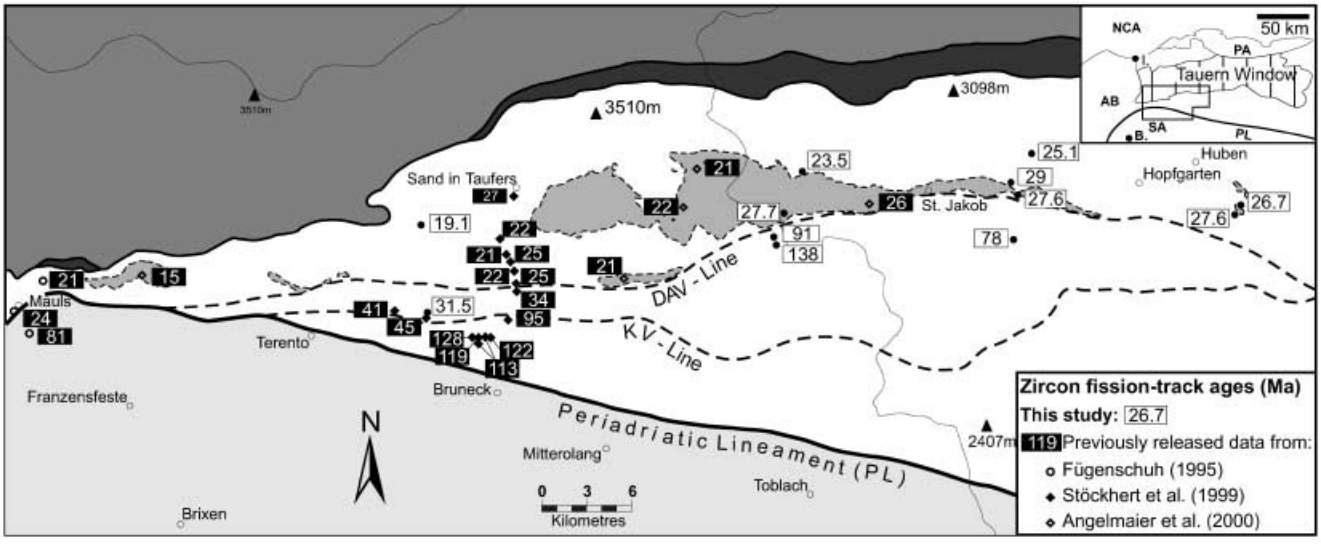

Fig. 5 Compilation of published and new zircon fission-track ages (see *insert*)

cooling during exhumation. To the south of the DAV Line, the similarity of the Rb/Sr and K/Ar white-mica ages obtained from various ortho- and paragneisses suggests rapid Late Variscan cooling at about 300 Ma. Two pegmatoid samples from south of the DAV Line yielded ages of around 190 Ma. Close concordance of the ages determined from a mica fraction of ≥350 µm suggests that they represent true cooling of silicic melts invading the Austroalpine basement during Early Jurassic times. Rejuvenation of these micas seems less likely because at least for the more western sample K/Ar- and Rb/Sr-biotite cooling ages from the surrounding area point to higher ages. Up to now, no Early Jurassic pegmatites have been reported from the Austroalpine basement south of the Tauern Window. At least the pegmatites that occur to the north of the DAV Line are constrained by Rb/Sr methods to be Permian in age (Borsi et al. 1980; Stöckhert 1984). However, the occurrence of Late Triassic pegmatites is reported by Sanders et al. (1996) from the Orobic basement of the Southern Alps.

Regional distribution of Rb/Sr- and K/Ar-biotite cooling ages

The K/Ar-biotite cooling ages obtained excellently fit the age pattern observed in former investigations (Borsi et al. 1979; Hammerschmidt 1981; Prochaska 1981). Cooling ages north of the DAV Line increase from around 17 Ma at the Rensen Pluton in the west to 27 Ma at the western end of the Rieserferner Pluton (Fig. 4). Further east, the increase in ages becomes less important. In the region of the eastern end of the Rieserferner Pluton and near the Isel Valley ages rise abruptly to val-

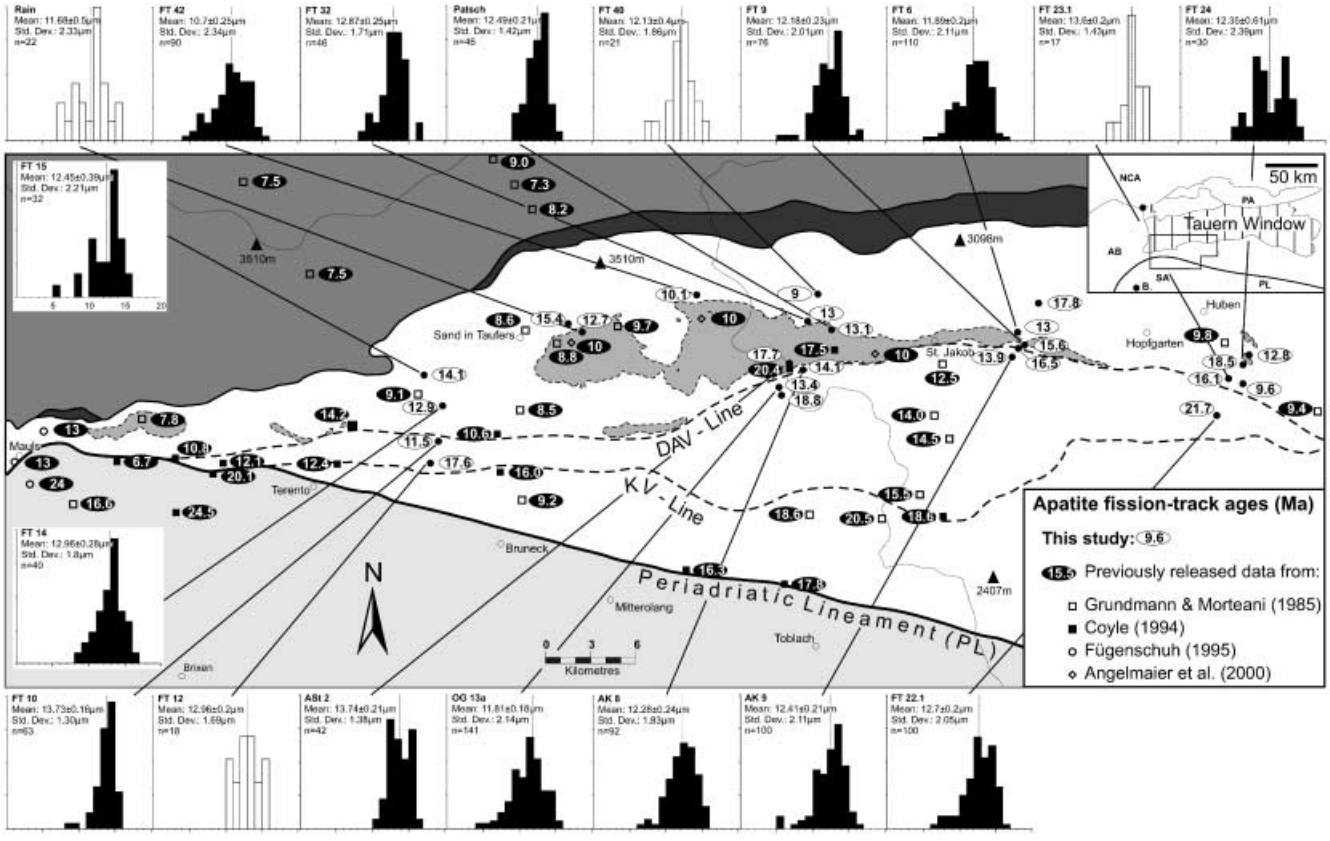

Fig. 6 Compilation of published and recent apatite fission-track data (see *insert*). Also given are track-length histograms of confined horizontal tracks in apatite. Distributions shown in outline represent small numbers (n<22) of measured track-lengths

Table 1 Compilation of the obtained K/Ar ages of muscovites and biotites. K_2O analyses of the standard mineral HD–B1 (Fuhrmann et al. 1987) were interspersed, with the sample material as a control of experimental technique. Errors on measured ages were calculated according to the error propagation of Gaussian Law, combining individual uncertainties from K_2O dual analysis, 1% general error of ^{40}Ar analysis, argon isotopic ratios and spike calibration. The quoted error complies with 95% of the confidence level (2σ). Ar – isotopic abundance; 40 Ar: 99.6000%; 38 Ar: 0.0630%; 36 Ar: 0.3370%. Spike – isotopic composition; 40 Ar: 0.0099980%; 38 Ar: 99.9890000%; 36 Ar: 0.0009998%. Decay constants (1 year^{-1}): lambda e: 5.810E-11; lambda β: 4.962E-10; lambda tot: 5.543E-10. Potassium; 40 K: 0.011670%; K_2O/K: 0.8302. Standard temperature pressure (STP); 0 °C; 760 mmHg; normal atmosphere (DIN 1343); 273.15 K; 1,013.25 mbar. Molar volume; (ml): 22413.8. Atomic weight (g mol^{-1}): tot Ar: 39.9477; 40 Ar: 39.9624; tot K: 39.1027

Sample		Spike (No.)	K_2O (Wt%)	40 Ar* (nl g^{-1}) STP	40 Ar* (%)	Age (Ma)	2s-error (Ma)	2s-error (%)
AK 8	Muscovite	2429	10.79	21.44	90.64	60.6	±1.3	2.1
AK 9	Muscovite	2487	10.67	70.05	95.10	193.0	±4.1	2.1
FT 10	Muscovite	2482	10.95	35.33	95.77	97.4	±2.1	2.2
FT 12	Muscovite	2437	10.73	111.99	98.48	297.8	±6.7	2.2
FT 14	Muscovite	2439	10.87	36.31	94.94	100.8	±2.1	2.1
FT 15	Muscovite	2441	11.05	21.12	87.17	58.4	±1.4	2.4
FT 22-1	Muscovite	2431	10.99	70.68	98.01	189.2	±8.6	4.5
OG 10	Muscovite	2488	11.00	119.82	98.92	309.8	±6.3	2.0
OG 13a	Muscovite	2500	10.16	104.83	98.96	294.7	±6.0	2.0
FT 30	Muscovite	2615	10.51	29.58	96.97	299.7	±8.0	2.7
FT 20	Muscovite	2613	7.44	83.82	97.74	319.5	±7.9	2.5
AST 2	Biotite	2489	8.02	8.49	90.97	32.5	±0.9	2.8
BS 23	Biotite	2502	9.25	73.12	99.22	229.9	±4.9	2.1
FT 1	Biotite	2515	8.49	77.12	99.17	261.9	±5.6	2.1
FT 9	Biotite	2520	7.72	7.39	96.54	29.5	±0.9	3.1
FT 32	Biotite	2601	9.22	7.99	80.66	26.7	±0.7	2.6
Patsch	Biotite	2603	9.41	8.52	93.27	27.9	±0.7	2.5
Rain	Biotite	2605	9.55	8.47	90.46	27.3	±0.8	2.9

Table 2 Apatite (*A*) and zircon (*Z*) fission-track ages. Sample localities are indicated in Fig. 2. All samples have been treated using the external detector method. Number of counted grains is given in column 3. ρs and ρi are spontaneous and induced track densities respectively; number of counted tracks is given in parenthesis. $P(\chi^2)$ test (Galbraith 1981). $\rho s/\rho s$ is the mean ratio. Zircon ages were calculated with a ζ-value of 130.4±7.4 for dosimeter glass CN 1. Apatite ages were calculated with a ζ-value of 358.8±11.4 for dosimeter glass CN 5. All ages are mean ages (Galbraith and Laslett 1993)

Sample	Altitude (m a.s.l.)	Number of grains counted	SD track density $\times 10^4$ cm^{-2} (counted)	ρs/ρi (±2s)	ρs $\times 10^4$ cm^{-2} (counted)	ρi $\times 10^4$ cm^{-2} (counted)	$P(\chi^2)$ (%)	Age (Ma) (±2s)
AK 8 A	2420	21	111.7 (2406)	0.078±0.005	20.43 (367)	306.9 (5513)	1.4	14.1±1.1
AK 9 A	1600	18	104.2 (2406)	0.077±0.004	35.59 (355)	478.2 (4770)	94.8	13.9±0.8
ASt 2 A	2620	17	130.4 (2406)	0.077±0.004	16.82 (107)	222.6 (1416)	99.7	17.7±1.8
ASt 2 Z		18	42.57 (639)	1.024±0.033	954.5 (2412)	960.8 (2428)	14.3	27.7±1.4
FT 1 Z	2100	20	45.74 (639)	2.629±0.136	620.8 (951)	235 (360)	89.5	78±6
FT 4 A	2260	22	141.7 (2406)	0.093±0.010	10.74 (116)	177.2 (1963)	1.0	17.8±2.3
FT 4 Z		21	43.48 (639)	0.891±0.035	210.7 (1070)	237.5 (1206)	59.1	25.1±1.5
FT 6 A	1500	21	122.9 (2406)	0.069±0.006	23.9 (217)	407 (3696)	28.5	13±1
FT 6 Z		17	43.93 (639)	1.031±0.046	262.2 (737)	258 (725)	77.4	29.0±1.9
FT 8 A	1380	20	115.4 (2406)	0.084±0.007	16.69 (79)	209.2 (990)	98.2	16.5±2
FT 9 A	1340	22	145.3 (2229)	0.060±0.004	20.01 (258)	333.2 (4296)	34.8	15.6±1.1
FT 9 Z		20	45.29 (639)	0.938±0.025	779.2 (2782)	832.4 (2972)	58.5	27.6±1.3
FT 10 A	2220	17	96.72 (2406)	0.067±0.004	21.81 (364)	327.5 (5464)	33.2	11.5±0.7
FT 12 A	1580	29	149.8 (2229)	0.068±0.003	6.11 (126)	93.16 (1921)	100.0	17.6±1.7
FT 12 Z		20	46.19 (639)	1.048±0.045	481.2 (2130)	440 (1948)	0.1	31.5±1.9
FT 14 A	1920	22	137.9 (2406)	0.052±0.002	21.09 (302)	402.6 (5766)	99.5	12.9±0.8
FT 15 A	1325	22	119.2 (2406)	0.073±0.005	8.696 (217)	132 (3293)	62.4	14.1±1
FT 15 Z		24	41.22 (639)	0.719±0.038	269.1 (1120)	377 (1569)	3.6	19.1±1.2
FT 20 A	1480	17	145.4 (2406)	0.050±0.010	2.406 (24)	65.47 (653)	72.4	9.6±2
FT 22.1 A	1680	21	100.5 (2406)	0.114±0.008	36.78 (338)	303.5 (2789)	49.1	21.7±1.4
FT 23.1 A	1600	23	112.6 (2275)	0.086±0.007	23.07 (246)	289 (3082)	77.8	16.1±1.1
FT 24 A	1280	21	127.1 (2229)	0.083±0.006	10.43 (156)	128.7 (1924)	86.9	18.5±1.6
FT 24 Z		17	48.45 (639)	0.867±0.030	454.4 (2494)	518.6 (2846)	47.7	27.6±1.3
FT 26 A	800	16	136.2 (2229)	0.055±0.004	7.392 (56)	141.2 (1070)	99.8	12.8±1.8
FT 26 Z		20	44.38 (639)	0.927±0.024	486.6 (2823)	526.6 (3055)	57.9	26.7±1.3
FT 30 A	2150	21	134.2 (2406)	0.078±0.005	13.77 (220)	176.4 (2819)	94.7	18.8±1.4
FT 30 Z		20	47.10 (639)	4.510±0.221	1026 (1857)	225.5 (408)	89.6	138±9
FT 32 A	1950	23	92.48 (2275)	0.089±0.008	14.68 (278)	187.2 (3543)	14.5	13.0±0.9
FT 32 Z		20	39.41 (639)	0.925±0.052	351.3 (1623)	377.7 (1745)	0.1	23.5±1.5
FT 40 A	1800	20	104.4 (2229)	0.051±0.004	13.70 (164)	284.3 (3403)	92.5	9.0±0.7
FT 41 A	1575	20	99.82 (2229)	0.118±0.018	3.31 (41)	38.51 (477)	75.2	15.4±2.5
FT 42 A	2000	19	95.28 (2229)	0.062±0.005	16.75 (246)	285.8 (4199)	18.4	10.1±0.8
OG 13a A	1900	20	140.7 (2229)	0.057±0.004	39.39 (276)	740.8 (5191)	88.2	13.4±0.9
OG 13a Z		16	47.55 (639)	3.057±0.183	1466 (3050)	500.8 (1042)	3.2	91±6
Patsch A	1630	23	108.9 (2229)	0.070±0.004	17 (221)	253.3 (3293)	94.4	13.1±1.0
Rain A	1280	21	122.5 (2229)	0.060±0.003	8.741 (146)	150.9 (2520)	99.1	12.7±1.1

ues of between 47 and 59 Ma. Borsi et al. (1978) postulated that westward younging reflects the variation of the erosion level caused by tilting of the crustal segment north of the DAV Line around a N–S axis after late Alpine metamorphism. Furthermore, they argued that high Rb/Sr ages from the easternmost end of the studied area are not related to the amount of tilting because it seems most likely that those ages reflect the partial resetting of earlier cooling. The trend towards higher biotite cooling ages continues further to the east across the Isel Valley (Hoke 1990).

Additionally, younging towards the north is well established. Cooling ages decrease from 30 Ma in the south to 17 Ma next to the Tauern Window. Borsi et al. (1978) argued that this rejuvenation of biotite cooling ages is the result of Upper Oligocene–Lowermost Miocene regional re-heating. A different approach to explain this decrease in ages is the difference in exhumation rates between the Tauern Window (Von Blanckenburg et al. 1989) and the Austroalpine basement to the south, resulting in a rotation around an E–W axis.

Noteworthy are K/Ar-biotite cooling ages of about 30 Ma directly to the north of the DAV Line. Well constrained ages in the region of the eastern end of the Central Rieserferner (ASt 2 – 32.5±0.9 Ma) match within error the recalculated Rb/Sr whole rock isochron of 31±3 Ma by Müller et al. (2000). The rather abrupt decrease in cooling ages from 30 to 27 Ma within a few hundred metres cannot easily be explained by crustal rotations, but may be the result of bent isotherms caused by the juxtaposition of relatively hot basement rocks north of the DAV Line against the colder southern block.

The Austroalpine basement south of the DAV Line is well characterised by Late Variscan Rb/Sr- and K/Ar-biotite cooling ages (Fig. 4). The sharp jump from Alpine ages in the north to Variscan ages in the south

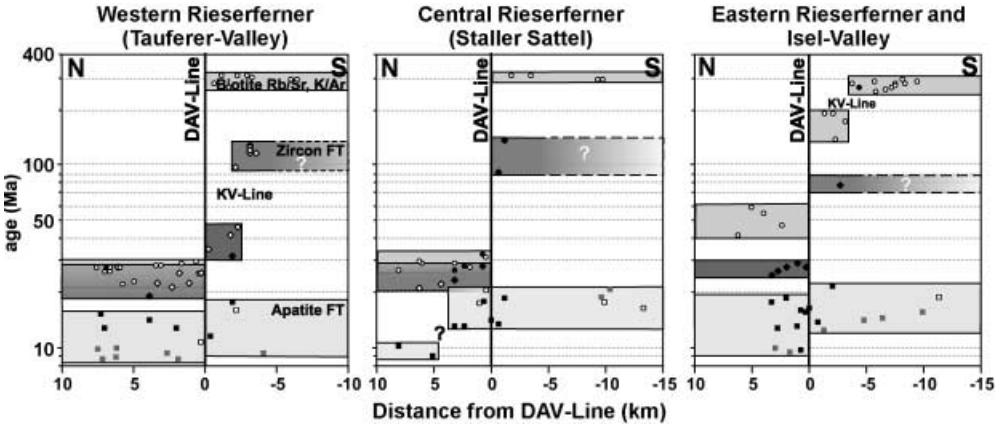

Fig. 7 Presentation of K/Ar- and Rb/Sr-biotite ages as well as zircon and apatite fission-track ages across the DAV Line from the three selected areas shown in Fig. 2. The variability of apatite fission-track ages in a similar range to both sides of the DAV Line support no constraints on the vertical displacement across the DAV Line from 22 Ma onwards. A marked decrease in apatite fission-track ages in the north of the Central Rieserferner reflects the northward younging direction towards the Tauern window. From the scarce data is not clear whether this trend is smooth or stepped. Zircon fission-track ages and K/Ar- and Rb/Sr-biotite ages clearly point to the role of the DAV Line (and also KV Line) during the Oligocene. Also, note the slight westward younging of all age groups in the north of the DAV Line. *Squares* apatite fission-track data; *diamonds* zircon fission-track data; *circles* K/Ar- and Rb/Sr-biotite data. *Filled symbols* represent new data from this study, whereas *open symbols* refer to the published data set (cf. Figs. 3, 4, 5 and 6). The *grey squares* represent the somewhat younger apatite fission-track ages from Grundmann and Morteani (1985) and Angelmaier et al. (2000)

emphasises the role of the DAV Line during the Alpine cycle (cf. Fig. 7).

Regional variation in FT-ages

Among the 25 investigated samples, 11 samples yielded both zircon and apatite, 13 samples were suitable for apatite dating and 1 sample for zircon dating only. The number of dated grains ranged between 16 and 29. Track length measurements of confined horizontal tracks were performed for 18 apatite samples. For all other apatite samples, the number of horizontal confined tracks was too low to be presented. Analytical data are given in Table 1. The regional distribution of ages is depicted in Figs. 5 and 6. The available data allow for the construction of a continuous cooling (exhumation) path from 350 °C (K/Ar white mica) to 90 °C (apatite fission track).

In the block to the north of the DAV Line, the newly obtained zircon fission-track ages fit the previously proven westward younging direction (Fügenschuh 1995; Stöckhert et al. 1999; Angelmaier et al. 2000). Ages of around 22 Ma between the Western Rieserferner and the Rensen Pluton increase towards 29 Ma in the eastern part of the study area (Fig. 5). The later clearly reflect cooling after alpine greenschist facies metamorphism. To the south of the Central Rieserferner, across the DAV Line, zircon fission-track ages strongly increase to Cretaceous ages whereas, further west, two marked jumps in zircon fission-track ages across the DAV Line and the KV Line are documented (Stöckhert et al. 1999; cf. Fig. 7).

Apatite fission-track data in the investigated area range between 9 and 22 Ma, complying with the previously ascertained apatite fission-track ages by Coyle (1994). Furthermore, ages obtained from the westernmost samples are consistent with the trend given by Fügenschuh (1995). Data published by Grundmann and Morteani (1985) and preliminary data by Angelmaier et al. (2000) are systematically younger than the results mentioned above (Fig. 6 and 8). Taking sample elevation into account, this difference is partly reduced because samples from Grundmann and Morteani (1985) are mostly taken at lower elevations. Yet, both data sets lack a clear correlation of age with altitude, most probably because of late faulting. Thus, the fission-track data cannot be reliably normalised to a topographic reference level. Nevertheless, the difference of the ages between the Rensen Pluton (7.8 Ma) and the Isel valley (9.8 Ma) is comparable with the new results. As it turns out, the calculated exhumation differences will be equivalent (see below).

Along a W–E-oriented profile, a weak tendency can be seen for increasing apatite fission-track ages towards the Isel valley (Figs. 6 and 8). In the east, ages increase markedly from the north of the Rieserferner Pluton towards the south across the DAV Line. In the N–S direction a weak, southward increase in age across the DAV Line is observed (Fig. 7). Because the available data show a large scatter in ages, the calculation of a vertical displacement on the base of apatite fission-track ages, as speculated by Coyle (1994), seems to be highly tentative. Additionally, apatite fission-track ages strongly decrease in the north of the Central Rieserferner (Staller Sattel, Fig. 7), continuous with the northward younging of ages within the Tauern window. Single grain ages of all counted apatites (Fig. 9) display a weak tendency for younger ages in the north. However, the oldest single grain ages were obtained in the northern block as well.

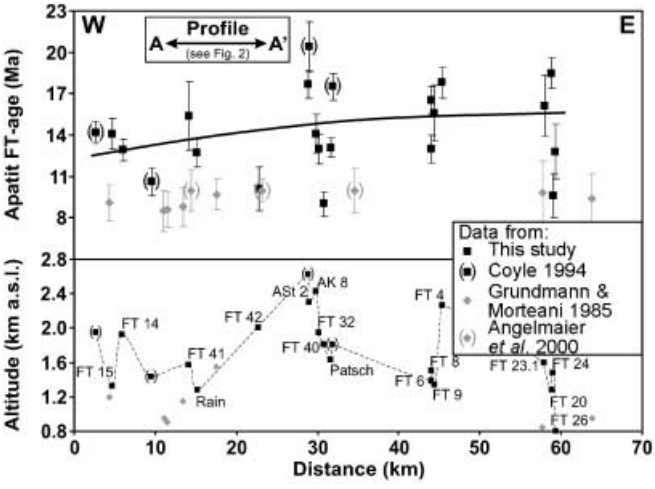

Fig. 8 *Top* Apatite fission-track ages along a W–E profile to the north of the DAV Line (*A–A'* in Fig. 2). *Bottom* Sample numbers from this study and their elevation. An arrogated age vs altitude relationship is only partly satisfied. The samples FT 42 and FT 40 from the north of the Rieserferner Pluton are continuous with the younging of ages towards the Tauern Window. Note that the fission-track ages from Grundmann and Morteani (1985) and Angelmaier et al. (2000) do only insufficiently fit the new data and previous data from Coyle (1994). These data are not included for the rough approximation of a trend-line

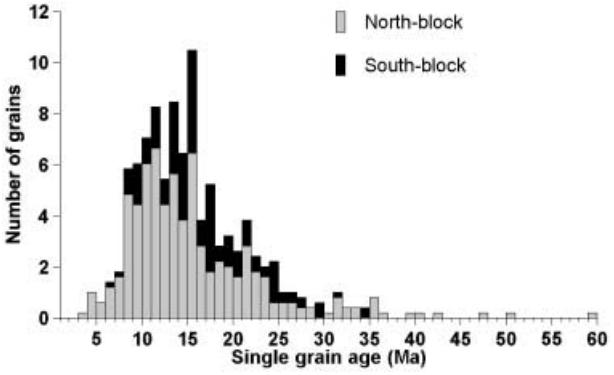

Fig. 9 Histogram of apatite single grain fission-track ages compiled from all newly obtained ages. A weak tendency for slightly older ages south of the DAV Line can be seen. Note that the youngest as well as the oldest single grain ages have been found in the northern block

Thermal history and constraints on the exhumation rates

Thermal modelling

In addition to the regional cooling caused by the exhumation of the Austroalpine basement, local re-heating of the basement occurs because of the emplacement of large volumes of magma that form a number of plutons (e.g. the Rieserferner Pluton). Therefore, the first important task to be solved in order to constrain the differential exhumation of the basement is to check whether ages are affected by contact metamorphic heating or reflect the joint exhumation of plutonic and basement rocks. Furthermore, the regional extension of the disturbance of isotherms is of interest in the context of an assumedly constant geothermal gradient.

In order to approximate the time interval it will take to cool the pluton down to the temperature of the host rock, numerical modelling was performed using a finite-difference approximation of mutually coupled equations describing the conduction of heat in a solid medium. For further details concerning the mathematical and numerical procedures of the used simulation code SHEMAT, the reader is referred to Clauser (1988) and Clauser and Villinger (1990).

The results of the numerical modelling of the cooling history of the magmas of the Rieserferner Pluton are only reasonable if these correlate to a large extent with the P–T conditions in the contact metamorphic envelope, constrained from metamorphic peak conditions deduced from mineral assemblages. Detailed investigations of the metamorphic contact envelope in the topmost sidewall in the south of the Central Rieserferner indicate six contact metamorphic zones (Cesare 1992, 1994, 1999). The 'second sillimanite' zone (Cesare 1992, 1999) at the contact of the pluton restricts the P–T conditions to 600–620 °C and a minimum pressure of 2.9 kbar. The extension of the observed contact metamorphic reactions is up to 1.5 km from the contact. Because investigations were undertaken in an area of a non-vertical contact plane, the actual width of the contact envelope is even less than 1.5 km. Considering the inclination of the pluton border, Mager (1985) observed a 230-m-wide contact zone perpendicular to the plutons surface. Also, former results from the northern contact area north of the Central Rieserferner point to a contact temperature of 630 °C and a rapid reduction of the temperature to 500 °C within 400 m distance (Prochaska 1981). The temperature of the unaffected country rock is estimated to 300–400 °C at the time of intrusion (Cesare and Hollister 1995; Cesare 1999).

Basic assumptions

The model is based on a 2-D vertical cross section of the Central Rieserferner and a N–S diameter of 7 km of the equatorial plane is taken. The geometry of the top half of the cross section is fairly well known from field observations and magnetic fabric patterns (Steenken et al. 2000). Because structural data supply only indirect information on the feeder zone, the deep structure of the model should be regarded as an approximation, following the model of the Bergell Pluton (Rosenberg et al. 1995). Surrounding crustal rocks are divided into a mainly metapsammopelitic 15-km-thick upper crust, which is underlain by a gabbroic composed lower crust, which takes up 5 km in the model.

A basal heat flow (Q_m) of 43 mW m^{-2} at the base of the model is calculated from an assumed surface heat flow (Q_s) of 70 mW m^{-2} (Della Vedova et al. 1995) ac-

cording to the formula by Midgley and Blundell (1997):

$$Q_m = Q_s - A_0 D + A_0 D e^{-\frac{d}{D}}$$

where d is the depth co-ordinate. A_0 is the surface radioactive heat production rate per unit mass and D is the length scale for the decrease in radioactive heat production with depth. In the model, the latter corresponds to the depth of the 15-km-thick upper crust, whose radioactive heat production rate is 2.44 μW m^{-3}, whilst the radioactive heat production rate in the lower crust is negligibly low. The radioactive heat production of the intrusive rocks of 3.29 μW m^{-3} is adopted from radiometric investigations of the Bergell Pluton (references in Čermák et al. 1982).

A large anisotropy in thermal conductivity of foliated rocks is known (Wenk and Wenk 1969; Langheinrich 1983), with the lowest thermal conductivity normal to the cleavage plane. Considering the concordant foliation of the country rock with respect to the plutons surface, a low value of 2.2 W m×K^{-1} is set as an average of typical metapsammopelitic crustal rocks (Čermák et al. 1982). The thermal conductivity within the intrusive rocks and lower crust is assumed to be isotropic and is set to 3.0 and 2.8 W m×K^{-1}, respectively. A permeability values of 1×10^{-18} m^2 is assigned to the metapsammopelitic upper crust, whereas the lower crust and the intrusive are set to a permeability value of 1×10^{-25} m^2.

Results of modelling

A first set of simulation runs was carried out in order to find a reasonable emplacement temperature of the magma sufficient to produce the observed contact metamorphic conditions very close to the contact at an ambient temperature of 360 °C. The results are summarised in Fig. 10a. It is indicated that a temperature of 600–620 °C at the contact (Cesare 1992, 1999) is held for less than 50,000 years after the emplacement of a 950 °C hot magma.

A different approach to estimate the emplacement temperature of the magma is based on the zircon saturation in a silicic melt (Watson and Harrison 1983). The Zr content in the granitoids of the Rieserferner Pluton ranges from 47 to 150 ppm (Bellieni et al. 1984; Schönhofer 1999), which leads to a melt temperature estimate of 761 °C for the early tonalitic precursors of the pluton, decreasing to 669 °C for the most fractionated granitic samples. The discrepancy of about 200 °C between the modelled melt temperature and the zircon saturation estimate may be the result of magma convection during the emplacement, where hot magma is recurrently transported next to the border of the pluton. Also porous flow of the remaining melt above the solidus may produce the observed contact metamorphic temperatures, even with the lower magma temperature indicated by the zircon saturation thermometer. However, a similarly high emplacement temperature was modelled from contact paragenesis for the Ardara Pluton (NW Ireland) that intruded at a depth corresponding to about 2.5 kbar. From ambient temperatures of about 300 °C and a contact temperature of 660 °C a magma temperature of 1000 °C was inferred (Paterson and Vernon 1995). Also, Scaillet et al. (1997) reported relatively high magma emplacement temperatures for high level intrusions.

Further uncertainties arise from synintrusive tectonic process that could not be taken into account by the model. Temperature loss during magma ascent, as well as synintrusive thinning of the plutonic roof (Rosenberg et al. 2000; Steenken et al. 2000), are important aspects of the emplacement of the Rieserferner Pluton. Taking synintrusive shortening into account it is difficult to constrain ambient temperatures before contact metamorphism because of vertical mass displacement. John and Blundy (1993) reported about 68% syn-emplacement shortening in the country rock of the southern Adamello massive. Paterson and Vernon (1995) conclude from porphyroblast-matrix relationships that expansion of magma chambers is usually less than 30%. In the event of country rock shortening, ambient temperatures may tend to the upper end of the predicted temperature interval between 300 and 400 °C (Cesare 1994, 1999).

As it turns out, starting the modelling at 950 °C will mark the uppermost limit of the emplacement temperature and, therefore, the maximum time interval it will take to balance the temperature of the pluton with its host. A marked thermal anomaly persists up to 0.5 Ma after the intrusion, whereas country rock and pluton are cooled to approximately the same temperatures after 2 Ma, indicating that K/Ar-biotite as well as Rb/Sr-biotite cooling ages at 4 Ma after the emplacement reflect regional cooling rather than contact metamorphic cooling. The difference in radioactive heat production between intrusive and country rock will lead to a little temperature difference only. This effect diminishes towards higher levels.

Comparing the width of the contact metamorphic envelope around the Rieserferner Pluton obtained from field investigations (see above) with the modelled temperature disturbance of isotherms in the host rock a large degree of concordance is indicated. However, modelled temperatures at the onset of the different contact metamorphic zones are too low to produce the observed metamorphic assemblages. A possible reason for this deficiency may be the result of a more complex intrusion

Fig. 10 Temperature development in the contact envelope of the Rieserferner Pluton assuming a **a** single relatively fast ascending magma pulse, and **b** a pulsed magma ascent within a time interval of 50,000 years (for simplicity of modelling two pulses are simulated only). In the latter case the propagation of the contact aureole increases compared with the intrusion of a single magma batch, whereas at the contact the temperatures are not raised. In both cases, the magma cools down to the temperatures of the country rock within 2 Ma. A weak thermal anomaly persists because of the higher radioactive heat production of the plutonic rocks. The *white profile line* marks the temperature profile in Fig. 11 ▶

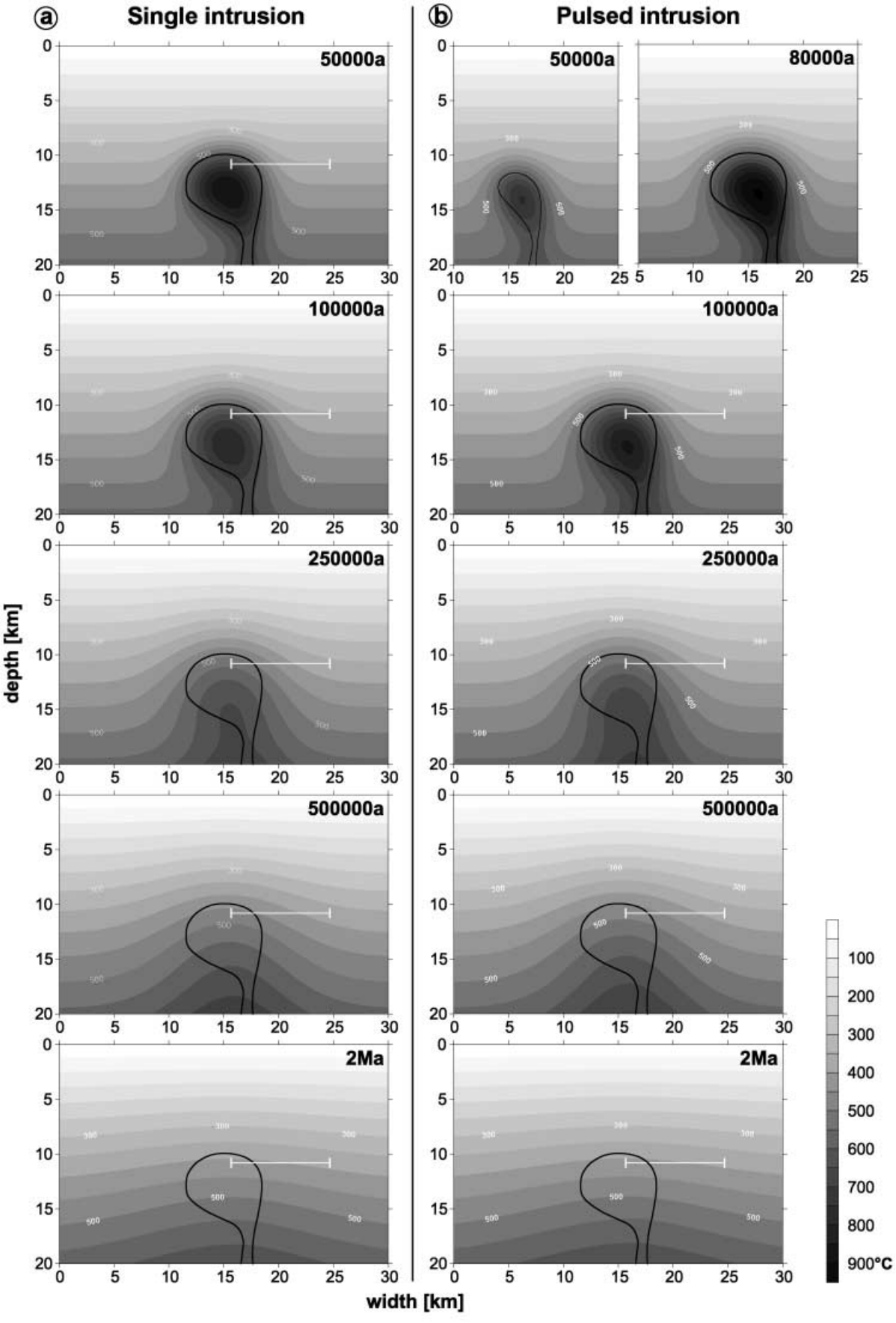
a
Single intrusion
b
Pulsed intrusion
50000a
80000a
100000a
250000a
500000a
2Ma
depth [km]
width [km]
100
200
300
400
500
600
700
800
900°C

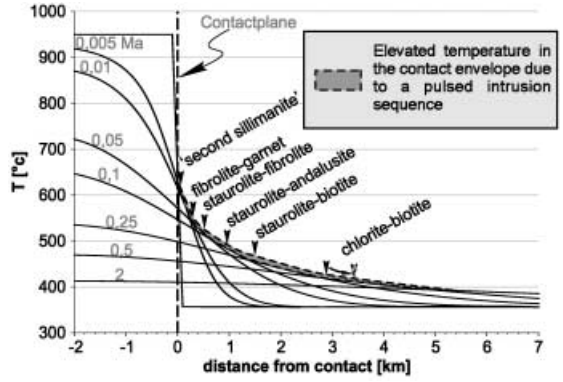

Fig. 11 Detailed aspect of the temperature propagation through contact during the emplacement of the Rieserferner Pluton. *Black arrows* mark the onset of the observed contact metamorphic zones in the metapelitic country rock. The *grey field* with the *dashed outline* shows the effect of the temperature development in the contact aureole for a pulsed magma ascent. The raised temperature approximates the required temperatures for the observed contact metamorphic reactions. Note that the onset of chlorite formation will start more distant to the contact

sequence comprising different magma pulses. Structural observations indicate a normal zoning of the pluton, suggesting the piercing of a second pulse close to the plutons centre. Because the magmatic foliation cross-cuts internal contacts between the petrologic subunits (Steenken et al. 2000), the intrusion of the later magma batches has to take place at temperatures markedly above the solidus of the first magma batch. Cooling down to sub-solidus temperatures of a smaller magma batch will constrain the time interval to 50000 years between two pulses (Fig. 10b). In case of the relatively small magma volume of the Rieserferner Pluton, the modelling results for a single or pulsed intrusion vary only slightly. In the case of the mentioned restrictions, the modelling will only be able to show general variations in the expansion of the contact aureole, but is not sufficient to account for a special intrusion sequence in case of the Rieserferner Pluton. Because the temperature of the second pulse will not be significantly higher than the first pulse, no higher temperatures at the contact are reached. However, a pulsed intrusion will cause a less steep temperature decrease towards the outer contact aureole, shifting temperatures to a more reasonable value to produce the observed metamorphic reactions (Fig. 11).

Petrological evidence for the beginning of contact metamorphism, characterised by the growth of fresh biotite and chlorite at temperatures above 420 °C, is hard to constrain because both minerals belong to the greenschist facies Alpine metamorphic assemblage within the pelitic rocks. The models point to the appearance of new chlorite and biotite within a distance of 3–3.5 km from the contact.

Exhumation of the Austroalpine basement

Following the blocking temperature concept (e.g. Dodson 1973), the cooling of a metamorphic area of uniform deformation history can be easily assessed by the application of different geochronological dating methods. Exhumation rates issuing from the cooling history are calculated in two different ways: (1) the mineral pair method (Wagner et al. 1977) utilises different blocking temperatures of minerals and/or isotope systems in the same sample; and (2) the altitude-dependence method applies the same dating method (commonly apatite fission-tracks) to several samples from unequal altitude (Wagner et al. 1977; Fitzgerald and Gleadow 1990). In both cases, exhumation is calculated from

$$\text{exhumation rate} = \frac{\Delta z}{\Delta t}$$

where Δz is the vertical distance between two samples, either calculated using an ‘estimated’ static and constant geothermal gradient or measured directly, and Δt is the age difference.

In particular, the mineral pair method is highly dependent and, therefore, largely limited by assumptions related to the geothermal gradient. Further, isotherms are affected by high exhumation rates (as, for example, recorded in the Tauern window; Von Blanckenburg et al. 1989) leading to heat advection reducing the spacing of isotherms (Mancktelow and Grasemann 1997). The altitude dependence method, on the other hand, is depending on the homogeneity of the exhumed rock body. This precondition is hardly met in the investigated area as indicated by the poor (and sometimes inverse) correlation of age with altitude (cf. Fig. 7).

Track lengths distributions of confined horizontal tracks provide further information on the thermal history (Gleadow et al. 1986; Green et al. 1989). Most samples yielded uniform distributions and the shortened mean track lengths of 11.7–13.7 µm (Fig. 6) point to cooling at moderate rates comparable with the undisturbed basement type of Gleadow et al. (1986). The shortest mean track lengths are recorded by samples (FT 6, FT 42 and OG 13a), whose distributions are more of ‘mixed type’ according to Gleadow et al. (1986). The only sample that yielded a bimodal track-lengths distribution (FT 24) is weakly constrained because of the low number of measured confined horizontal tracks (n=30).

More detailed information on the cooling history is gained from fission-track annealing models. For this purpose the ‘Monte Trax’ software is utilised (Gallagher 1995), which deals with the single grain ages and track length distribution. The procedure to find a best fit model for the T–t path is based on an initial stochastic search (genetic algorithm) combined with a maximum likelihood approach, whose theoretical background is described by Gallagher (1995). Modelling is restricted because track annealing is highly sensitive to the crystal chemistry of the dated apatites and, therefore, to the chosen annealing model. In the following, uniform track length predictions will be presented choosing the annealing model for the Durango apatite of Laslett et al. (1987). An upper limit for the modelled time interval is given by the zircon fission-track ages obtained. Because

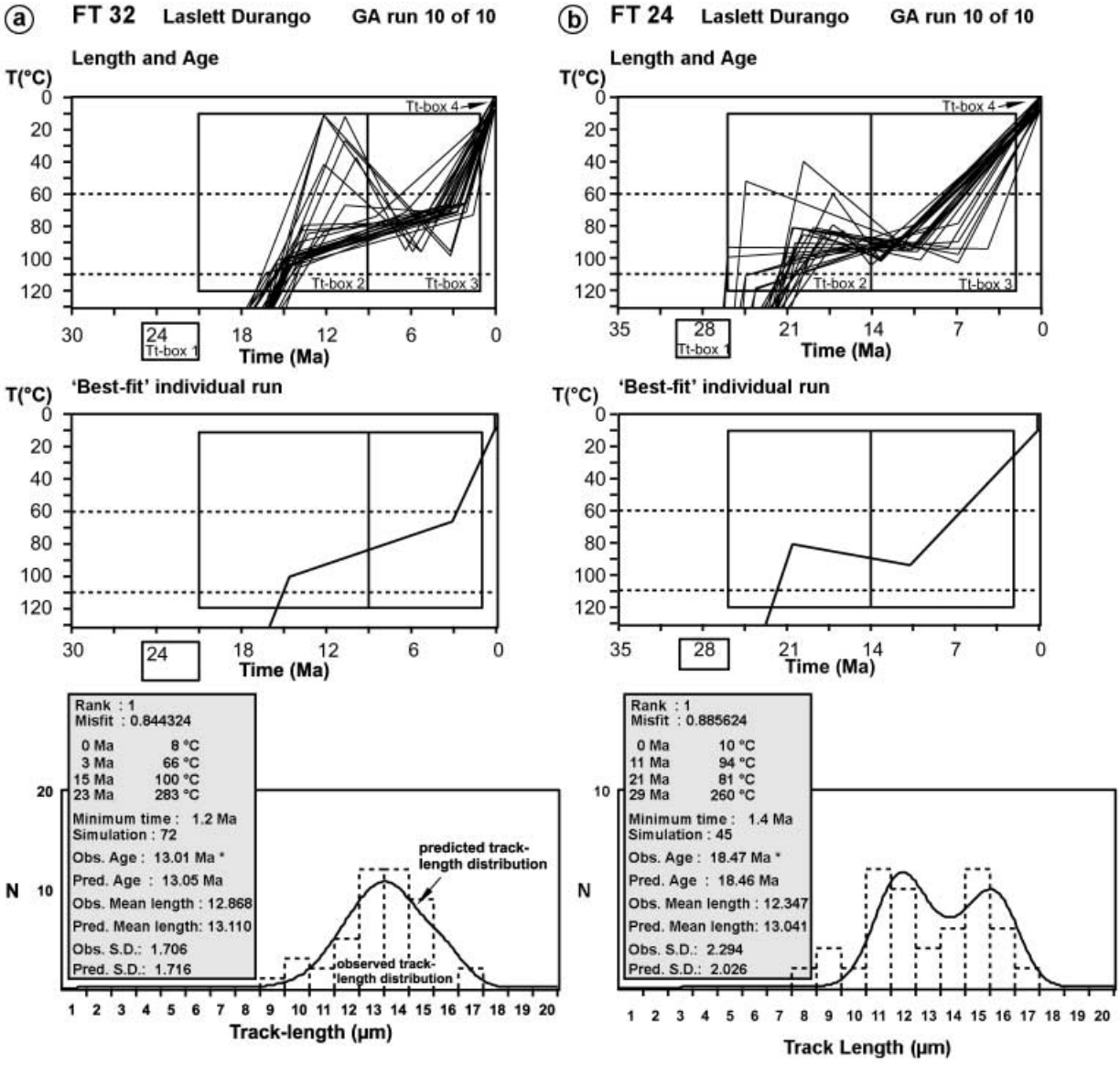

Fig. 12 Genetic algorithm (*GA*) simulation for two apatite fission-track samples representative for the **a** central and **b** eastern part of the studied area. Ten GA runs with 100 simulations each. The *top figures* present only those T–t paths that fit the observed length and age data. It is indicated that most of the simulated exhumation paths pass straight through the PAZ, whereas only a few exhumation paths arrogate a more complex exhumation history. The four *lower figures* show the best runs after 1100 simulations and the correspondence between the observed and predicted track-length distribution. The exhumation path for **a** sample FT 32 passes relatively straight the PAZ whereas, for **b** FT 24, the exhumation history is more discontinuous. This is in agreement with the lower exhumation rates in the eastern part of the studied area

the observed track-length distributions are rather uniform, sample FT 32 was chosen as representative. Therefore, the starting point at 23±2 Ma and 240±60 °C is taken for modelling the exhumation path of sample FT 32, whereas the end point is constrained by recent surface conditions. The T–t space is subsequently divided into further 'T–t boxes' covering the confined time and temperature range. Initial models are based on several 'T–t boxes' that confirm the exhumation history. Further models were performed on a reduced number of two 'T–t boxes' to allow more freedom to vary the generated T–t histories, but all the models are only able to generate a simple track length distribution where the observed track length distribution and the modelled distribution are in agreement (Fig. 12a). Because the modelled time interval is rather short, a simple T–t history is reasonable for the exhumation history of the Rieserferner Pluton and its country rock. The best fit models for the observed ages and track length distribution generally indicate that the basement, after cooling below the 110 °C isotherm, undergoes for about 10 Ma weak only cooling during passing the PAZ followed by a more rapid cooling during final exhumation. Also, the bimodal track length distribution of sample FT 24 from the easternmost part of the study area could be explained by a simple division of the confined T–t space. With the exception of three cooling paths that fit the length and single grain age model

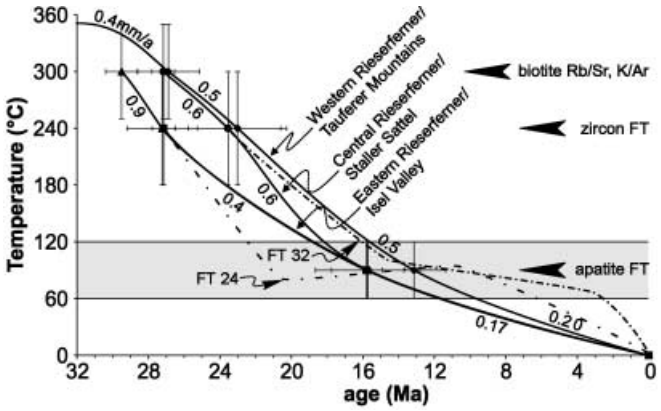

Fig. 13 Cooling history of the Austroalpine basement in the north of the DAV Line and direct constraints on the amount of exhumation assuming an average geothermal gradient of 28 °C/km. The standard deviation of the summarised age data from this study and previous data (Borsi et al. 1979; Coyle 1994; Stöckhert et al. 1999) for the different exhumation paths is presented by *horizontal error bars*. *Vertical error bars* reflect uncertainties from closure temperatures of the different isotopic systems. Also indicated are the modelled cooling paths based on single grain ages and track-length distribution for the samples FT 32 and FT 24. For the variability of these cooling paths see Fig. 12. In contrast to the asymptotic cooling history, by using the apparent fission-track age only, a more complex cooling history is conceivable when the modelled cooling paths are taken into account

data, the suggested cooling path is characterised by relatively constant temperatures between 21 and 11 Ma in the mid range of the PAZ (Fig. 12b). During final exhumation, cooling rates are slightly reduced in comparison to sample FT 32.

It is also indicated by the models based on the track length distributions and single grain ages that the apparent fission-track ages represent minimum ages of cooling through the 120 °C isotherm. However, the difference to the modelled probable cooling age is demonstrably small, and of the order of the error of the mean of regional groups of samples (Fig. 13). Generally its relevance to the cooling path seems negligible.

Furthermore, it seems highly questionable to transfer the constrained latest part of the cooling path directly into exhumation rates because the more shallow levelled isotherms are strongly effected by the high topographic relief in the studied area. A more detailed discussion of the final cooling history of the samples should be based on a higher sample density.

In order to reveal the complete exhumation history of the Rieserferner Pluton, isotope systems with higher closure temperature have to be incorporated. Also, the Rb/Sr isochron of the Rieserferner Pluton should be integrated into the cooling history of the Austroalpine basement. Thus, the large gap between eo-Alpine metamorphism at 102 Ma (Stöckhert 1984) and the biotite cooling ages that range from 16 to 30 Ma is bridged. Because the assumed closure temperature for the K/Ar system in muscovite of 350±50 °C equals the temperatures for the basement at the time of pluton emplacement (Cesare 1999), no cooling takes place between the closure of the K/Ar-muscovite system and the emplacement of the pluton. Onset of cooling, therefore, is constrained by the emplacement of the Rieserferner Pluton. The cooling rates decrease asymptotically towards final exposure. Assuming an average geothermal gradient of 28° km^{-1} (Bellieni and Visona 1981) cooling rates are directly converted into exhumation rates, labelled on the various cooling paths in Fig. 13. Moderate exhumation rates in the range of 0.4 and 0.6 mm year^{-1} are bracketed between the intrusion age and the apparent apatite fission-track ages, whereas final exhumation took place with an exhumation rate of about 0.2 mm year^{-1}. Also indicated in Fig. 13 are the modelled 'best-fit' cooling paths for two apatite fission-track samples (Fig. 12). It is indicated that the modelled cooling path for the Western and Central Rieserferner is in close accordance with the constrained cooling path using the apparent fission-track age only. The increased difference between the apparent fission-track age and the modelled cooling age below the 120 °C isotherm further east leads to the possible interpretation that exhumation took place at similar rates as those for the Western and Central Rieserferner until 21 Ma, followed by a period of constant temperatures. However, the comparison between the variability of the modelled cooling path (Fig. 12b) and the mean of the error of the regional age groups (Fig. 13) shows a wide overlap. Therefore, both interpretations may be reasonable.

Because the simple conversion of cooling rates into exhumation rates depends on several assumptions mentioned above a different approach is used following the method outlined by Von Blanckenburg et al. (1989), by placing time marks on the P–T loop. Unfortunately, in the area of interest, this method is handicapped because the temperature range of well-constrained metamorphic conditions scarcely matches the temperature range covered by the applied dating methods. However, adopting the P–T loop from Cesare (1999), established within the pelitic country rock of the Central Rieserferner, exhumation rates could be constrained in a similar way (Fig. 14). As in the previous approach, negligibly small exhumation rates prior to the emplacement emerge, whereas during and after magma emplacement exhumation rates rise abruptly towards 1.7 mm year^{-1}, and asymptotically decrease towards final exhumation. To check whether a reasonable exhumation history for the Austroalpine basement could be reconstructed, simple modelling adopting the algorithm described by Mancktelow and Grasemann (1997) was performed. The model is confined to a temperature of 1,300 °C at 100 km depth. Radiometric heat production within the upper 30 km of the model exponentially decays to 1/e of the surface value of 2.80×10^{-6} W m^{-3}. The starting point for exhumation, as defined by muscovite K/Ar ages of 102 Ma, is at a depth of 12.4 km. Adopting the exhumation rates estimated from the P–T loop, it is indicated that, except for the emplacement of the Rieserferner Pluton, neither K/Ar-biotite nor fission-track ages fall into the right tempera-

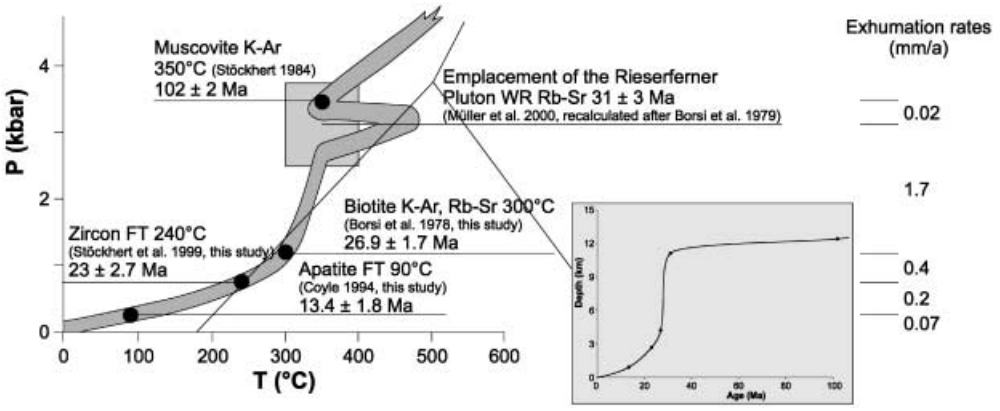

Fig. 14 Time markers placed on the P–T path established by Cesare (1999). Calculated exhumation rates decrease asymptotically starting with the intrusion of the Rieserferner Pluton. The most striking difference to the calculated exhumation history from the mineral pair method (Fig. 13) is the relatively high exhumation rate of 1.7 mm year^{-1} bracketed between the intrusion of the Rieserferner Pluton and the closure temperature for the K/Ar-biotite system. The *small inset* shows the exhumation path in a depth versus time diagram

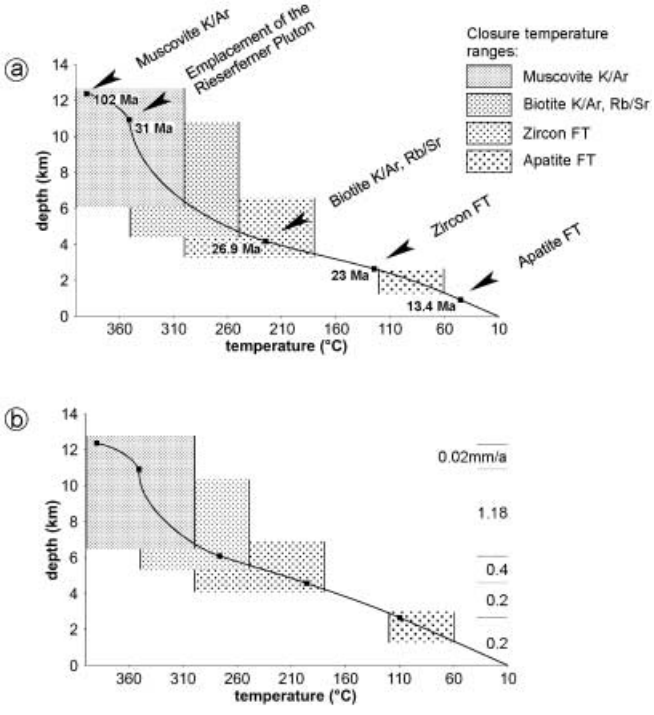

Fig. 15a, b Modelled P–T–t paths for the Western Rieserferner and its surrounding Austroalpine basement. In **a** the modelled path is based on the estimated exhumation rates obtained from the P–T path of Cesare (1999). It is evident that the calculated exhumation path would not allow the placement of the K/Ar-biotite and all fission-track data in their assumed closure temperature interval. **b** Modified exhumation path with reduced exhumation rates just after the magma emplacement and, consequently, their higher exhumation rates during final exposure in order to fit the obtained data. *Dotted bars* indicate the presumed closure temperature intervals for the applied isotopic systems

ture range (Fig. 15a). Obviously this problem arises from increased exhumation rates following the emplacement of the Rieserferner Pluton at 31±3 Ma, which are followed by reduced exhumation rates during later stages of exhumation.

Modifying the exhumation path in order to fit the postulated temperature ranges for the different dating methods, high initial exhumation rates have to be reduced to 1.2 mm year^{-1}, consequently exhumation rates during the final exhumation increase up to 0.2 mm year^{-1} (Fig. 15b). Furthermore, resulting exhumation rates approximate the exhumation rates calculated from the mineral pair method within error. Hence, it is assumed that cooling rates directly respond to the variable exhumation within the Austroalpine basement to the north of the DAV Line.

Detailed investigations on the Alpine PT evolution further east are lacking (Schönhofer 1999), preventing a comparison between the two methods. Low cooling rates in the eastern part of the study area will allow us to convert those directly into exhumation rates within geological error. As it turns out, variations in the cooling history north of the DAV Line may directly correspond to the differences in the exhumation history. Comparing the obtained cooling ages within and outside the Rieserferner Pluton it is suggested that both underwent the same exhumation history (Fig. 16).

Detailed evaluation of the different isotope systems shows that the array of more or less constant ages progresses westwards during the cooling history. This may indicate that the area affected by tilting was reduced. Assuming an average geothermal gradient of 28 °C km^{-1} a differential vertical displacement between the Western Rieserferner and the upper Defereggen Valley of about 2.2 km is indicated by K/Ar-biotite and zircon fission-track ages suggesting an east-side-down rotation of approximately 5°. The rotation is nearly completed before the rocks reach the PAZ for apatite fission-track ages. After passing the PAZ for apatite 0.5 km of vertical difference were levelled only (Fig. 16).

A slightly different rotational history of the Rieserferner Pluton is archived when the modelled apatite fission-track cooling paths are incorporated. Following this approach, the exhumation of the Rieserferner Pluton

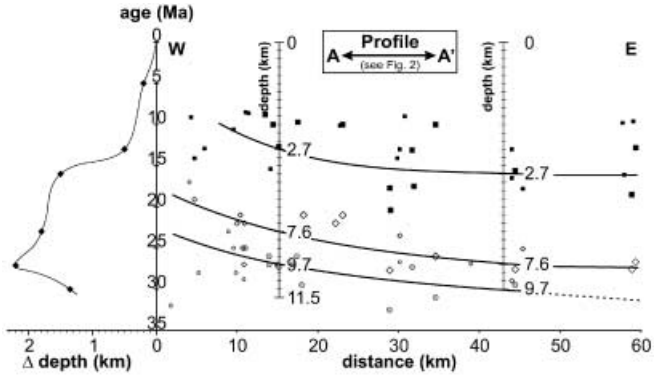

Fig. 16 Age vs. distance diagram for new and compiled Rb/Sr-, K/Ar-biotite (*black filled squares*), zircon (*open diamonds*) and apatite (*grey filled dots*) fission-track ages. The difference in *symbol size* corresponds to the origin of samples, either from the Oligocene intrusives (*tall symbols*) or the Austroalpine basement (*small symbols*). Note that the two depth scales are individually scaled, corresponding to the depth of an averaged age group at given time, assuming an average geothermal gradient of 28 °C. The diagram to the left exhibits the estimated exhumation difference (Δ depth) between the Western and Eastern Rieserferner

took place at similar exhumation rates, but ceased at different times just after passing the 120 °C isotherm. As it turns out, the vertical difference between the Eastern and Western Rieserferner remains until the eastern part enters the apatite PAZ. The east-side-down rotation is initiated by the enduring exhumation of the Western Rieserferner. Final exposure takes place at uniform exhumation rates.

In view of the numerous brittle structures with at least marked strike-slip offset (Schönhofer 1994, 1999) observed within the investigated area, the fission-track data obtained so far are still too scattered to decide whether the observed age trend is smooth or caused by brittle discrete faults adding up to the total displacement observed.

Conclusion

Careful evaluation of different thermochronological systems can be a useful tool in the determination of exhumation rates in orogenic belts, provided that exhumation is slow (<1 mm year^{-1}) and will not shift the depth of isotherms in a geologically significant manner (Mancktelow and Grasemann 1997). Additional uncertainties arise from potentially inhomogeneous cooling of the basement because of numerous brittle faults with minor vertical displacement. Because this effect is hard to reckon, the estimation of exhumation rates is rather *ad hoc* and, because no associated error can be given, values should be regarded as a rough approximation only.

Low cooling rates north and south of the DAV Line allow their direct transformation into exhumation rates. To the north of the DAV Line, exhumation rates are continuously decreasing from nearly 1 mm year^{-1} bracketed between the intrusion of the Rieserferner Pluton and the closure temperature for K/Ar and Rb/Sr system in biotite towards 0.2 mm year^{-1} during final exposure. Highest exhumation rates south of the DAV Line are confined by Variscan Rb/Sr and K/Ar mica cooling ages overlapping within error.

Although zircon fission-track ages north and south of the DAV Line still mark a vertical displacement, a smooth pattern in apatite fission-track ages across the DAV Line points to a common exhumation history (see also Coyle 1994; Stöckhert et al. 1999).

The difference between the apparent fission-track age and the modelled cooling history may lead to a slightly different rotational exhumation history of the Rieserferner Pluton. However, the final orientation of the pluton is not affected.

One main task to solve is the implication for fabric elements and outcrop pattern of the Oligocene Rieserferner Pluton. Similarities between this pluton and the akin Bergell Pluton regarding the development of a narrow, elongated tail, may suggest an analogous emplacement and exhumation style (Rosenberg et al. 1995). This conception cannot be maintained on the basis of the thermochronometric data set obtained in this study, indicating that the deepest part of the pluton corresponds with the Western Rieserferner, whereas the narrow tail along the Defereggen Valley represents the highest intrusion level. The initial vertical difference as indicated by K/Ar- and Rb/Sr-biotite cooling ages is 2.2 km. A similar trend was found from hornblende-barometry data (Albertz et al. 1999). The vertical difference is nearly completely balanced prior to passing PAZ for apatite fission-tracks where a exhumation difference of 0.5 km is left over.

This observation is in good agreement with the developed emplacement model for the Rieserferner Pluton (Steenken et al. 2000). The appearance of highly evolved granitic magmas along the core axis of the tail of the Rieserferner Pluton, enclosed by quartz–dioritic compositions, suggests that those intrusions belong to the latest stage during the intrusion history. They may even comprise independent intrusions conflated prior to final solidification.

Acknowledgements The authors would like to thank Nico Froitzheim and an anonymous colleague for the detailed and helpful reviews. Fission-track preparation and dating was kindly supported by Stefan Schmid, who granted unconfined access to the laboratory facilities at the Geology Department of Basel. We are in debt to M. Raab for his constructive criticism in our fission-track work. The K/Ar dating was performed by Klaus Wemmer and his laboratory team at the Göttinger Zentrum für Geowissenschaften, which should be highly acknowledged. Additionally, we thank Hans Ahrend in memorial. Numerous field excursions and fruitful discussions with R. Schönhofer and B. Schulz are highly acknowledged. W. Schnabel and the Geologische Bundesanstalt (Austria/Vienna) granted access to the forest paths of the Austrian part of the Rieserferner area. A. St. would like to thank the Niedersächsische Graduiertenförderung and the Deutscher Akademischer Austauschdienst for their scholarships and S.S. thanks the German Science Foundation for a Heisenberg – Fellowship (Si 438/10-1.2).

Appendix

Sample preparation and experimental procedure

Between 1 and 10 kg of suitable sample material was taken for the separation of micas, zircon and apatite. Sample preparation processed in the usual manner by crushing and sieving. For enrichment of zircon and apatite, the grain fraction smaller 40 µm was further treated by Wilfley table, magnetic separation, heavy liquids (bromoform, methylene iodide) and hand picking. During the whole procedure, samples were never heated above 35 °C to avoid any decrease in number and size of fission-tracks, particularly in apatite.

The residual coarse fraction was handled for mica enrichment using a mica-jet as described by Wemmer (1991) followed by standard techniques as for the apatite and zircon enrichment. The purity of the mica separates was >99%. Finally purified micas were ground in pure alcohol to remove altered rims that might have suffered a loss of Ar or K.

The argon isotopic composition was measured in a Pyrex glass extraction and purification line coupled to a VG 1200 C noble gas mass spectrometer, operating in static mode. The amount of radiogenic ^{40}Ar was determined by isotope dilution method using a highly enriched ^{38}Ar spike from Schumacher, Bern (Schumacher 1975). The spike was calibrated against the biotite standard HD-B1 (Fuhrmann et al. 1987). The age calculations are based on the constants recommended by the IUGS quoted in Steiger and Jäger (1977).

Potassium was determined in duplicate by flame photometry using an Eppendorf Elex 63/61. The samples were dissolved in a mixture of HF and HNO_3 according to the technique of Heinrichs and Herrmann (1990). CsCl and LiCl were added as an ionisation buffer and internal standard, respectively. The analytical error for the K/Ar age calculations is given at a 95% confidence level (2σ). Details of argon and potassium analyses for the laboratory in Göttingen are given in Wemmer (1991).

For polishing of the fission-track sample, material apatites were embedded in Araldite M whereas zircons were pressed in PFA Teflon. The etching of the apatites takes 35 s in 10% HNO_3 at 20 °C. Zircons were etched in a KOH–NaOH eutectic melt at 210 °C for 8 h at least. Muscovites used as external detectors (EDM, Naeser 1979) for all mounts and dosimeter glasses were treated with 40% HF at 20 °C for 45 min.

Counting was performed on a Zeiss optical microscope equipped with a calibration tablet run by the program Langstage (Dumitru 1993). Apatites were counted under dry conditions with a magnification of 1×10×100 while zircons were counted with a total magnification of 1.6×10×100 using oil immersion. Ages were calculated using a zeta-value (Hurford and Green 1983) of 359±11 (Durango, CN 5) for apatite and 130±7 (Fish Canyon Tuff CN1) for zircon.

References

Albertz M, Rosenberg C, Möbus C, Handy M (1999) The roof of the Rieserferner Pluton: implications for syntectonic magma ascent and emplacement along crustal scale shear zones. The origin of granites and related rocks, IVth Hutton Symposium 73

Angelmaier P, Dunkl I, Frisch W (2000) Altersprofile aus dem Zentralabschnitt der Transalp-Traverse (Ostalpen): neue K/AR-, Zirkon- und Apatitspaltspurendatierungen. Terra Nostra, Schriften Alfred–Wegener–Stiftung 5:4

Barth S, Oberli F, Meier M (1989) U–Th–Pb systematics of morphologically characterized zircon and allanite; a high-resolution isotopic study of the Alpine Rensen Pluton (northern Italy). Earth Planet Sci Lett 95(3–4):235–254

Becke F (1892) Petrographische Untersuchungen am Tonalit der Rieserferner. Tschermarks Mineral Petrol Mitt 13:379–433

Bellieni G, Visona D (1981) Metamorphic evolution of the Austroalpine schists outcropping between the intrusive masses of Vedrette di Ries (Rieserferner) and Cima di Vila (Zinsnock) (Eastern Alps, Italy). N Jb Geol Paläont Mh 10:586–602

Bellieni G, Peccerillo A, Poli G, Fioretti A (1984) The genesis of late Alpine plutonic bodies of Rensen and Monte Alto (Eastern Alps); inferences from major and trace element data. N Jahrb Min Abh 149(2):209–224

Bonneville A, Capolsini P (1999) THERMIC; a 2-D finite-element tool to solve conductive and advective heat transfer problems in Earth sciences. Computer Geosci 25(10):1137–1148

Borsi S, Del Moro A, Sassi FP, Zirpoli G (1973) Metamorphic evolution of the austridic rocks to the south of Tauern Window (Eastern Alps). Radiometric and geo-petrologic data. Mem Soc Geol It XII:549–571

Borsi S, Del Moro A, Sassi FP, Zanferrari A, Zirpoli G (1978) New petrologic and radiometric data on the alpine history of the austridic continental margin south of the Tauern Window (Eastern Alps). Mem Inst Geol Min Univ Padova 32:1–17

Borsi S, Del Moro A, Sassi FP, Zirpoli G (1979) On the age of the Vedrette di Ries (Rieserferner) massif and its geodynamic significance. Geol Rundsch 68:41–60

Borsi S, Del Moro A, Sassi FP, Visona D, Zirpoli G (1980) On the existence of Hercynian aplites and pegmatites in the lower Aurina Valley (Ahrntal, Austrides, Eastern Alps). N Jahrb Mineral Monatsh 11:501–514

Čermák V, Huckenholz H-G, Rybach L, Schmid R, Schopper JR, Schuch M, Stöffler D, Wohlenberg J (1982) Physical properties of rocks. In: Angenheister G (ed) Landolt-Börnstein, numerical data and functional relationships in science and technology. Group V: geophysics and space research. Springer, Berlin Heidelberg New York, pp 315–371

Cesare B (1992) Metamorfismo di contatto di rocce pelitiche nell' aureola di Vedrette di Ries (Alpi Orientali – Italia). Atti Tic Sc Terra 35:1–7

Cesare B (1994) Hercynite as the product of staurolite decomposition in the contact aureole of Vedrette di Ries, Eastern Alps, Italy. Contrib Mineral Petrol 116(3):239–246

Cesare B (1999) Multi-stage pseudomorphic replacement of garnet during polymetamorphism. 1: Microstructures and their interpretation. J Metamorph Geol 17(6):723–734

Cesare B, Hollister S (1995) Andalusite-bearing veins at Vedrette di Ries (Eastern Alps, Italy); fluid phase composition based on fluid inclusions. J Metamorph Geol 13:687–700

Clauser C (1988) Untersuchungen zur Trennung der konduktiven und konvektiven Anteile im Wärmetransport in einem Sedimentbecken am Beispiel des Oberrheingrabens. Fortschr Ber VDI. Reihe 19/28

Clauser C, Villinger H (1990) Analysis of conductive and convective heat transfer in a sedimentary basin, demonstrated for the Rheingraben. Geophys J Int 100(3):393–414

Coyle DA (1994) The application of apatite fission track analysis to problems in tectonics. PhD Thesis, La Trobe University, Bundoora, Victoria

Della Vedova B, Lucazeau F, Pasquale V, Pellis G, Verdoya M (1995) Heat flow in the tectonic provinces crossed by the southern segment of the European Geotraverse. In: Balling N, Decker ER (eds) Heat flow and thermal regimes of continental lithosphere. Tectonophysics 244(1–3):57–74

Dodson MH (1973) Closure temperature in cooling geochronological and petrological systems. Contrib Mineral Petrol 40(3): 259–274

Dumitru TA (1993) A new computer-automated microscope stage system for fission-track analysis. Nucl Track Radio Measure 21:575–580

England PC, Molnar P (1990) Surface uplift, uplift of rocks, and exhumation of rocks. Geology (Boulder) 18(12):1173–1177

Fitzgerald PG, Gleadow AJW (1990) New approaches in fission track geochronology as a tectonic tool; examples from the Transantarctic Mountains. In: Durrani SA, Benton EV (eds) Proceedings of the 6th international fission track dating workshop. Nucl Track Radio Measure 17(3):351–357

Froitzheim N, Conti P, van Daalen M (1997) Late Cretaceous, synorogenic, low-angle normal faulting along the Schlinig Fault (Switzerland, Italy, Austria) and its significance for the tectonics of the Eastern Alps. Tectonophysics 280(3–4):267–293

Fügenschuh B (1995) Thermal and kinematic history of the Brenner area (Eastern Alps, Tyrol). PhD Thesis, Eidgenössisch Technische Hochschule Zürich

Fügenschuh B, Mancktelow MS, Seward D (2000) Cretaceous to neogene cooling and exhumation history of the Oetztal–Stubai basement complex, eastern Alps: a structural and fission track study. Tectonics 19(5):905–918

Fuhrmann U, Lippolt HJ, Hess JC (1987) Examination of some proposed K–Ar standards: $^{40}Ar/^{39}Ar$ analyses and conventional K–Ar data. Chem Geol (Isot Geosci Sect) 66:41–51

Galbraith RF (1981) On statistical models for fission-track counts. Math Geol 13:471–438

Galbraith RF, Laslett GM (1993) Statistical models for mixed fission-track ages. Nucl Tracks Radiat Measure 21:459–470

Gallagher K (1995) Evolving temperature histories from apatite fission-track data. Earth Planet Sci Lett 136(3–4):421–435

Gleadow AJW, Duddy IR, Green PF, Lovering JF (1986) Confined fission track lengths in apatite; a diagnostic tool for thermal history analysis. Contrib Mineral Petrol 94(4):405–415

Green PF, Duddy IR, Laslett GM, Hegarty KA, Gleadow AJW, Lovering JF (1989) Thermal annealing of fission tracks in apatite. 4: Quantitative modelling techniques and extension to geological timescales. Chem Geol (Isot Geosci Sect) 79(2): 155–182

Grundmann G, Morteani G (1985) The young uplift and thermal history of the central Eastern Alps (Austria/Italy), evidence from apatite fission track ages. Jb Geol B-A 128:197–216

Guhl M, Troll G (1987) Die Permotrias von Kalkstein im Altkristallin der südlichen Deferegger Alpen (Österreich). Jahrb Geol B-A 130:37–60

Hammerschmidt K (1981) Isotopengeologische Untersuchungen am Augengneis vom Typ Campo Tures bei Rain in Taufers, Südtirol. Mem Sci Geol Mineral Univ Padova 34:273–300

Heinrichs H, Herrmann AG (1990) Praktikum der Analytischen Geochemie. Springer, Berlin Heidelberg New York

Hoke L (1990) The Altkristallin of the Kreuzeck Mountains, SE Tauern Window, Eastern Alps; basement crust in a convergent plate boundary zone. Jahrb Geol B-A 133(1):5–87

Heller F (1980) Paleomagnetic evidence for late Alpine rotation of the Lepontine area. In: Rybach L, Lambert A (eds) Symposium on the Alpine geotraverses with special emphasis on the Basel–Chiasso profile. Eclo Geol Helv 73(2):607–618

Hurford AJ, Green PF (1983) The zeta age calibration of fission-track dating. Chem Geol 41(4):285–317

John B, Blundy JD (1993) Emplacement-related deformation of granitoid magmas, southern Adamello massif, Italy. Geol Soc Am Bull 105:1517–1541

Kazmer M, Kovacs S (1985) Permian–Paleogene paleogeography along the eastern part of the Insubric-Periadriatic lineament system; evidence for continental escape of the Bakony–Drauzug Unit. Acta Geol Hung 28(1–2):71–84

Kleinschrodt R (1978) Quartzkorngefügeanalyse im Altkristallin südlich des westlichen Tauernfensters. Erlanger Geol Abh 114:1–82

Kosakowski G, Kunert V, Clauser C, Franke W, Neugebauer HJ (1999) Hydrothermal transients in Variscan crust; paleo-temperature mapping and hydrothermal models. Tectonophysics 306:325–344

Langheinrich G (1983) Waermeleitfaehigkeit anisotroper Gesteine. Geol Rundsch 72(2):541–588

Laslett GM, Green PF, Duddy IR, Gleadow AJW (1987) Thermal annealing of fission tracks in apatite. Chem Geol (Isot Geosci Sect) 65(1):1–13

Mager D (1985) Geologische und petrographische Untersuchungen am Südrand des Rieserferner Plutons (Südtirol) unter Berücksichtigung des Intrusionsmechanismus. PhD Thesis, Universität Erlangen, Nürnberg

Mancktelow NS, Grasemann B (1997) Time-dependent effects of heat advection and topography on cooling histories during erosion. Tectonophysics 270(3–4):167–195

Mancktelow NS, Stöckli DF, Grollimund B, Müller W, Fügenschuh B, Viola G, Seward D, Villa IM (2001) The DAV Line and Periadriatic fault system in the Eastern Alps south of the Tauern window. Int J Earth Sci 90(3):593–622

Mann A, Scheuvens D (1998) Structural investigation of the northern contact of the Rieserferner Plutonic Complex (Eastern Alps) – first results. Terra Nostra, Schriften der Alfred-Wegener-Stiftung 98:62

Midgley JP, Blundell DJ (1997) Deep seismic structure and thermo-mechanical modelling of continental collision zones. In: Touret JLR, Austrheim H (eds) Collisional orogens; zones of active transfer between crust and mantle. Tectonophysics 273(1–2):155–167

Most T (1997) Gefügekundliche Untersuchungen und Fluid-/Gesteinswechselwirkungen der Kataklasite der Defereggen-Antholz-Vals (DAV)-Linie N′ des Staller Sattels und S′ von St. Veit in Defereggen. Diploma Thesis, Institut für Geologie und Dynamik der Lithosphäre, Göttingen, Germany

Müller W, Mancktelow NS, Meier M (2000) Rb–Sr microchrons of synkinematic mica in mylonites; an example from the DAV Fault of the Eastern Alps. Earth Planet Sci Lett 180(3–4): 385–397

Naeser CW (1979) Thermal history of sedimentary basins; fission-track dating of subsurface rocks. In: Scholle PA, Schluger PR (eds) Aspects of diagenesis. Soc Econ Paleontol Mineral Spec Publ 26:109–112

Parrish RR (1983) Cenozoic thermal evolution and tectonics of the Coast Mountains of British Columbia; 1: fission track dating, apparent uplift rates, and patterns of uplift. Tectonics 2(6): 601–631

Paterson SR, Vernon RH (1995) Bursting the bubble of ballooning plutons; a return to nested diapirs emplaced by multiple processes. Geol Soc Am Bull 107(11):1356–1380

Prochaska W (1981) Einige Ganggesteine der Riesenfernerintrusion mit neuen radiometrischen Altersdaten. Mitt Ges Geol Bergbaustud Österr 27:161–171

Purdy JW, Jäger E (1976) K–Ar ages on rock forming minerals from the Central Alps. Mem Inst Geol Mineral Univ Padova 30:1–31

Rahn MK, Brandon MT, Batt GE, Garver JI (2002a) Zircon fission track annealing I. The temperature and time relationship between alpha and FT damage? Am Mineral (in press)

Rahn MK, Brandon MT, Batt GE, Garver JI (2002b) Zircon fission track annealing II. The ‘zero damage’ model? Am Mineral

Ratschbacher L, Frisch W, Linzer HG, Merle O (1991) Lateral extrusion in the Eastern Alps. Part 2: structural analysis. Tectonics 10(2):257–271

Rosenberg CL, Berger A, Schmid SM (1995) Observations from the floor of a granitoid pluton: inferences on the driving force of final emplacement. Geology 23(5):443–446

Rosenberg CL, Wagner R, Handy MR (2000) The roof of the Rieserferner Pluton: syntectonic magma ascent and emplacement along a crustal scale shear zones. 2nd International TRANSALP-Colloquium, programme abstracts no 20

Sanders CAE, Bertotti G, Tommasini S, Davies GR, Wijbrans JR (1996) Triassic pegmatites in the Mesozoic middle crust of the southern Alps (Italy); fluid inclusions, radiometric dating and tectonic implications. In: Schmid SM, Frey M, Froitzheim N, Heilbronner R, Stünitz H (eds) Alpine geology; proceedings of the second workshop. Eclo Geol Helv 89(1): 505–525

Sassi FP, Zanferrari A, Zirpoli G (1974) Some considerations on the south-Alpine basement of the Eastern Alps. N Jb Geol Paläont Mh 10:609–624

Scaillet B, Holtz F, Pichavant M (1997) Rheological properties of granitic magmas in their crystallization range. In: Bouchez JL, Hutton DWH, Stephens WE (eds) Granite: from segregation of melt to emplacement fabrics. Kluwer, Dordrecht, pp 95–112

Schmid SM, Aebli HR, Heller F, Zingg A (1989) The role of the Periadriatic Line in the tectonic evolution of the Alps. In: Coward MP, Dietrich D, Park RG (eds) Conference on Alpine tectonics. Geol Soc Spec Publ 45:153–171

Schönhofer R (1994) Geologische und petrographische Untersuchungen am Südrand des Rieserfernerplutons (Antholzer Tal, Südtirol). Diploma Thesis, Universität Erlangen, Nürnberg

Schönhofer R (1999) Das ostalpine Altkristallin der westlichen Lasörlinggruppe (Osttirol, Österreich): Kartierung, Stoffbestand und tektonometamorphe Entwicklung. Erlanger Geol Abh 130:1–128

Schulz B (1989) Jungalpidische Gefügeentwicklung entlang der Defereggen–Antholz–Vals-Linie, Osttirol, Österreich. Jahrb Geol B-A 132:775–789

Schulz B (1994) Microstructural evolution of metapelites from the Austroalpine basement north of Staller Sattel during pre-Alpine and Alpine deformation and metamorphism (Eastern Tyrol, Austria). Jahrb Geol B-A 137(1):197–212

Schulz B (1997) Pre-Alpine tectonometamorphic evolution in the Austroalpine basement to the south of the central Tauern window. Schweiz Mineral Petrol Mitt 77:281–297

Schumacher E (1975) Herstellung von 99.9997% ^{38}Ar für die ^{40}K/^{40}Ar Geochronologie. Geochron Chimia 24:441–442

Siegesmund S, Jelsma HA, Becker J, Davies G, Layer PM, van Dijk E, Kater L, Vinyu M (2001) Constraints on the timing of granite emplacement, deformation and metamorphism in the Shamva area, Zimbabwe. Int J Earth Sci (in press)

Steenken A, Siegesmund S, Heinrichs T (2000) The emplacement of the Rieserferner Pluton (eastern Alps, Tyrol): constraints from field observations, magnetic fabrics and microstructures. J Struct Geol 22(11–12):1855–1873

Steiger RH, Jäger E (1977) Subcommission on geochronology: convention on the use of decay constants in geo- and cosmochronology. Earth Planet Sci Lett 36:359–362

Stöckhert B (1984) K–Ar determinations on muscovites and phengites and the minimum age of the Old Alpine deformation in the Austridic basement south of the western Tauern Window (Ahrn valley, Southern Tyrol, Eastern Alps). N Jahrb Mineral Abh 150:103–120

Stöckhert B, Brix MR, Kleinschrodt R, Hurford AJ, Wirth R (1999) Thermochronometry and microstructures of quartz – a comparison with experimental flow laws and predictions on the temperature of the brittle–plastic transition. J Struct Geol 21:351–369

Stöckli D (1995) Tectonics SW of the Tauern window (Mauls area, Südtirol). Southern continuation of the Brenner Fault Zone and its interaction with other large fault structures. Diploma Thesis, ETH, Zürich

Von Blanckenburg F, Villa IM, Baur H, Morteani G, Steiger RH (1989) Time calibration of a PT-path from the western Tauern Window, Eastern Alps; the problem of closure temperatures. Contrib Mineral Petrol 101(1):1–11

Wagner GA (1972) The geological interpretation of fission track ages. Trans Am Nucl Soc 15:1–117

Wagner GA, Naeser CW, Hurford AJ, Gleadow AOW (1977) Fission-track dating of pumice from the KBS Tuff, East Rudolf, Kenya. Nature 267(5612):649

Watson EB, Harrison TM (1983) Zircon saturation revisited; temperature and composition effects in a variety of crustal magma types. Earth Planet Sci Lett 64(2):295–304

Wemmer K (1991) K/Ar-Altersdatierungsmöglichkeiten für retrograde Deformationsprozesse im spröden und duktilen Bereich – Beispiele aus der KTB-Vorbohrung (Oberpfalz) und dem Bereich der Insubrischen Linie (N-Italien). Göttinger Arb Geol Paläont 51:1–61

Wenk HR, Wenk E (1969) Physical constants of Alpine rocks (density, porosity, specific heat, thermal diffusivity and conductivity). Schweiz Mineral Petrol Mitt 49(2):343–357

Westphal M, Boschert S, Schumacher J (2002) The granulite-facies rocks of the Rogaland anorthosite complex in southwestern Norway: a thermal model. (in press)

Yamada R, Tagami T, Nishimura S, Ito H (1995) Annealing kinetics of fission tracks in zircon; an experimental study. Chem Geol 122(1–4):249–258

Zarske G (1985) Kartierung, Strukturgeologie und Petrologie im Altkristallin zwischen Erlsbach und Oberseitsee in den nordwestlichen Deferegger Alpen, Osttirol. Diploma Thesis, Insitut für Geologie und Paläontologie der Technischen Universität, Clausthal

Zimmermann R, Hammerschmidt K, Franz G (1994) Eocene high pressure metamorphism in the Penninic units of the Tauern Window (Eastern Alps); evidence from ^{40}Ar–^{39}Ar dating and petrological investigations. Contrib Mineral Petrol 117(2): 175–186